

1 **The future of Alpine Run-of-River hydropower production: climate change, environmental**  
2 **flow requirements, and technical production potential**

3

4 **Wechsler Tobias<sup>1,2,4</sup>, Stähli Manfred<sup>1,4</sup>, Jorde Klaus<sup>3,4</sup>, Zappa Massimiliano<sup>1,4</sup>, Schaeffli**  
5 **Bettina<sup>2,4</sup>**

6 *<sup>1</sup>Swiss Federal Institute for Forest, Snow and Landscape Research WSL, Zürcherstrasse 111, 8903 Birmensdorf,*  
7 *Switzerland*

8 *<sup>2</sup>Institute of Geography (GIUB) and Oeschger Centre for Climate Change Research (OCCR), University of Bern,*  
9 *Hallerstrasse 12, 3012 Bern, Switzerland*

10 *<sup>3</sup>KJ Consult, Ferdinand-Raunegger-Gasse 26, 9020 Klagenfurt, Austria*

11 *<sup>4</sup>Swiss Competence Center for Energy Research – Supply of Electricity (SCCER-SoE), Sonneggstrasse 5, 8092*  
12 *Zurich, Switzerland*

13

14 Correspondence: tobias.wechsler@wsl.ch

15 **Abstract**

16 Past studies on the impacts of climate change (CC) on Alpine hydropower production have  
17 focused on high-head accumulation power plants. We provide one of the first comprehensive,  
18 simulation-based studies on CC impacts on Alpine Run-of-River (RoR) production, also  
19 considering effects of environmental flow requirements and technical increase potential. We  
20 simulate future electricity production under three emissions scenarios for 21 Swiss RoR plants  
21 with a total production of 5.9 TWh a<sup>-1</sup>. The simulations show an increase in winter production (4%  
22 to 9%) and a decrease in summer production (-2% to -22%), which together lead to an annual  
23 decrease of about -2% to -7% by the end of the century. The production loss due to environmental  
24 flow requirements is estimated at 3.5% of the annual production; the largest low-elevation RoR  
25 power plants show little loss, while small and medium-sized power plants are most affected. The  
26 potential for increasing production by optimising the design discharge amounts to 8% of the  
27 annual production. The largest increase potential is related to small and medium-sized power  
28 plants at high elevations. The key results are: i) there is no linear relationship between CC impacts  
29 on streamflow and on RoR production; the impacts depend on the usable streamflow volume,  
30 which is influenced by the Flow Duration Curve, environmental flow requirements, and design  
31 discharge; ii), the simulated production impacts show a strong correlation (>0.68) with the mean  
32 catchment elevation. The plants at the highest elevations even show an increase in annual  
33 production of 3% to 23%, due to larger shares of precipitation falling as rain instead of snow.  
34 These general results are transferable to RoR production in similar settings in other Alpine  
35 locations and should be considered in future assessments. Future work could focus on further  
36 technical optimisation potential, considering detailed operational data.

37

38 **Keywords:** Hydropower, Run-of-River power plants, climate change, environmental flow,  
39 design discharge, Alps

40 **Abbreviations**

41	CC	Climate change
42	CH2018	Swiss climate change scenarios
43	WFD	Water Framework Directive
44	FDC	Flow Duration Curve
45	HP	Hydropower
46	HRU	Hydrological Response Unit
47	Hydro-CH2018	Swiss streamflow scenarios
48	IPCC	Intergovernmental Panel on Climate Change
49	PREVAH	PREcipitation streamflow EVApotranspiration HRU related model
50	RCM	Regional Climate Model
51	RCP	Representative Concentration Pathway
52	RoR	Run-of-River (power plant)
53	SRES	Special Report on Emissions Scenarios
54	WASTA	Swiss statistics on hydropower plants

55 **Notations**

56	$E$	Actual electricity production [MWh]
57	$E_e$	Production loss due to environmental flow requirements
58	$E_{opt}$	Production increases by optimising the design discharge
59	$F$	Simplified overall efficiency [ $\text{kg m}^{-2} \text{s}^{-2}$ ]
60	$H$	Hydraulic head [m]
61	$P$	Installed power [MW]
62	$Q_d$	Design discharge [ $\text{m}^3 \text{s}^{-1}$ ]
63	$T$	Time period

## 64 1 Introduction

65 Hydropower (HP) is a key renewable electricity source throughout the world (Gernaat et al. 2017;  
66 Schaefli et al. 2019; IHA 2020). This is especially the case in Alpine countries, where the  
67 topographic setting leads to high water input (Farinotti et al. 2012; Fatichi et al. 2015a) but also  
68 to locally high hydraulic heads. In the context of climate change (CC) impact assessment on HP  
69 production in Alpine countries, where CC is particularly strong (Köplin et al. 2010; Addor et al.  
70 2014; Fatichi et al. 2015b; BAFU 2021; Muelchi et al. 2021), there has been a strong focus on  
71 high-head accumulation production (Ranzani et al. 2018; Bombelli et al. 2019; Farinotti et al.  
72 2019; Schaefli et al. 2019), because of significant changes of the snow- and glacier-melt feeding  
73 these plants.

74 CC impact studies on Run-of-River (RoR) power plants are comparably rare (Hänggi and  
75 Weingartner 2012; Mohor et al. 2015; Wagner et al. 2017). This is critical because these plants  
76 typically have a very different turbine operation pattern compared to storage power plants. The  
77 International Energy Agency (IEA 2021) estimates, based on data from selected European  
78 countries (France, Germany, Portugal, Spain, Switzerland, Austria), that RoR operation is at full  
79 turbine capacity around 40% of the time, which is significantly greater than that of storage power  
80 plants (~15% of the time) and pumped storage power plants (~10% of the time).

81 Detailed CC impact studies on Alpine RoR electricity production based on catchment-scale  
82 streamflow projections generally conclude that future production will closely follow streamflow  
83 changes: a slight decrease in mean annual streamflow and a pronounced seasonal shift, with less  
84 streamflow in summer and more streamflow in winter (Bernhard and Zappa 2009; Köplin et al.  
85 2010; Addor et al. 2014; Brunner et al. 2019; Vázquez-Tarrío et al. 2019), with a corresponding  
86 decrease in summer production and an increase in winter production (Hänggi and Weingartner  
87 2012; Savelsberg et al. 2018). The change will be more pronounced at higher elevations,  
88 especially in catchments dominated by snow and glaciers (Hänggi and Weingartner 2012;

89 François et al. 2018). There is, however, no reason to assume a linear relationship between CC-  
90 induced changes in streamflow and corresponding changes in RoR electricity production (Wagner  
91 et al. 2017). François et al. (2018) showed, for northern Italy, that RoR electricity production in  
92 snow-dominated catchments can increase even though streamflow is expected to decrease.  
93 Indeed, impacts on electricity production crucially depend on the range of streamflow that is used  
94 for production, which in turn depends on the Flow Duration Curve (FDC; cumulative probability  
95 distribution of streamflow), the design discharge, and any water-use restrictions imposed for  
96 ecosystem protection (Basso and Botter 2012; Bejarano et al. 2019; Kuriqi et al. 2019; Yildiz and  
97 Vrugt 2019).

98 In addition, there are a few regional CC impact assessments that rely on a coarse representation  
99 of hydrology and simplified treatment of RoR production. For example, Savelsberg et al. (2018)  
100 set up a national-scale electricity market model for Switzerland including 400 HP plants (around  
101 300 of which are RoR power plants); they found a relatively large change in winter production  
102 compared with the change in streamflow and explained this by excess turbine capacities in winter  
103 and early spring that could be used for production under the future streamflow regime. The  
104 authors compared future scenarios with individual years in the past that were either dry, wet or  
105 average. Compared with the average year 2008, they simulated a future increase in annual  
106 production of 4%. Given the coarse resolution of the results, no detailed insights into the change  
107 in production along spatial gradients could be provided. Similarly, Totschnig et al. (2017) use a  
108 dynamic simulation model of the Austrian and German electricity, heating and cooling sectors in  
109 combination with CC scenarios; their model included around 400 RoR plants and simulated a  
110 reduction of 5.5% in the mean annual RoR production for Austria and Germany by mid-century  
111 under emission pathway A1B of the IPCC's Special Report on Emissions Scenarios (SRES), but  
112 without giving further insights into variables that might drive this change.

113 Existing studies on Alpine RoR electricity production give hardly an insight into how to transfer  
114 the obtained results to other locations. This seriously limits larger-scale projections of how CC will  
115 impact RoR production, despite the now well-known general tendencies in Alpine streamflow  
116 evolution. To our knowledge, there is a single study proposing an extrapolation of CC impacts on  
117 the entire Alpine region: Wagner et al. (2017) found an annual decrease of RoR production of  
118 8%, with a widespread increase in winter and decrease in summer. They used a simplified  
119 hydrological model with a monthly time step and a mixed approach to convert streamflow changes  
120 to electricity production, using a detailed model based on technical parameters for Austria and a  
121 simple linear model elsewhere. The underlying CC scenarios were based on scenarios that  
122 preceded the ones currently in use (SRES emission pathway A1B). These regional studies give  
123 clear indications of the general trend in RoR production in the Alpine region, but they cannot  
124 explain how the simulated changes might be modulated by local hydroclimatic, technical and  
125 operational specificities, and water use restrictions. Such restrictions exist for all types of RoR  
126 power plants, e.g. reserved flow for fish passability in the case of RoR plants built across streams.  
127 The water use restrictions can be even more important in case of so-called diversion power plants,  
128 where water is locally diverted to increase the hydraulic head. In this case, a certain amount of  
129 streamflow has to be maintained in the main river to satisfy further water use interests, such as  
130 irrigation, water supply, groundwater recharge, ecosystem demand, habitat connectivity, fish  
131 passage or sediment transport, and is defined as environmental flow (Anderson et al. 2015;  
132 Bejarano et al. 2019; Kuriqi et al. 2019; Calapez et al. 2021; Carolli et al. 2022).

133 Therefore, the aim of our study is to understand, based on hydrological simulations, how RoR  
134 electricity production could change under CC. We assess in detail the impacts on an annual and  
135 seasonal scale and analyse explanatory variables and their influence on RoR production. We  
136 simulate for the first time the transient RoR electricity production throughout the century using  
137 daily streamflow scenarios (BAFU 2021; Brunner et al. 2019). The main innovation lies in the

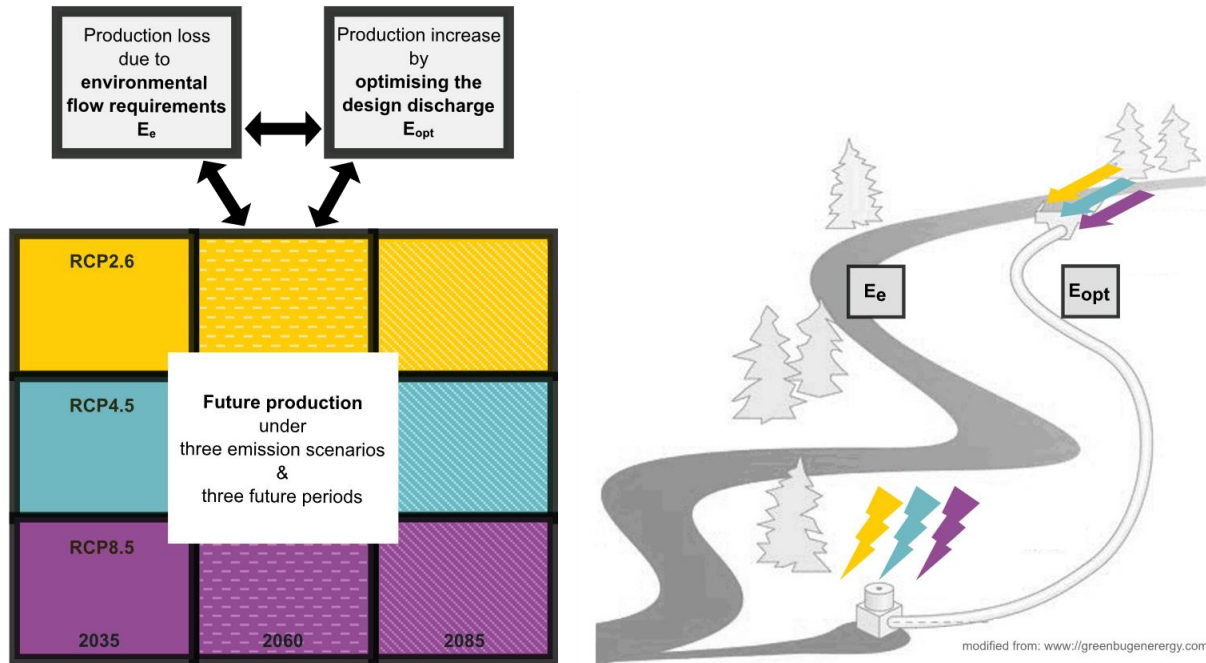
138 inclusion of both the environmental flow requirements and the technical optimisation potential,  
139 which modulate the RoR production. We use a comprehensive set of 21 RoR plants in  
140 Switzerland, representing different catchment sizes, streamflow regimes and infrastructure  
141 characteristics. The choice of Switzerland is relevant because of its general high share of HP and  
142 its pronounced variation in hydro-climatological regimes and in HP infrastructures within a small  
143 Alpine area. Accordingly, the results for the diverse RoR power plants presented here will be at  
144 least partly transferable to other Alpine regions.

## 145 2 Material and methods

### 146 2.1 General change assessment framework

147 The analysis framework applied in our study (Figure 1) is based on the comparison of current  
148 RoR production (reference period  $T_{ref}$ : 1981–2010) i) future production under climate change  
149 (CC); ii) production loss due to environmental flow requirements ( $E_e$ ); and iii) production increase  
150 potential resulting from an optimisation of the design discharge of the installed turbines ( $E_{opt}$ ). For  
151 the CC impact assessment, we use three future periods ( $T_1/2035$ : 2020–2049,  $T_2/2060$ : 2045–  
152 2074,  $T_3/2085$ : 2070–2099) and three emissions scenarios (RCP2.6: concerted CC mitigation  
153 efforts; RCP4.5: limited CC mitigation measures; and RCP8.5 no CC mitigation measures).

154 Given that we do not have exact observations of actual RoR production at these sites, the entire  
155 analysis is based on the hydrological production potential, i.e. the production that could  
156 theoretically be possible given the available streamflow and the power plant characteristics and  
157 environmental flow requirements (but not accounting for real-time turbine operations or shut-  
158 downs).



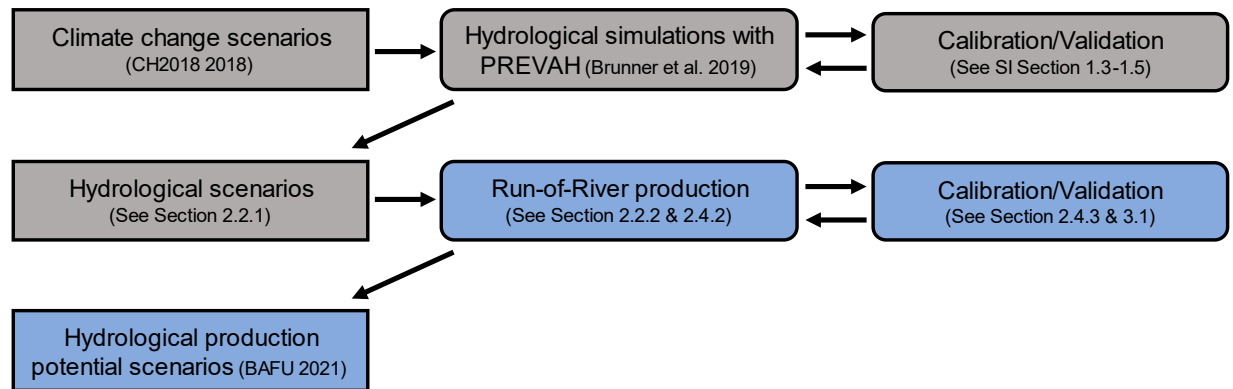
159  
160 *Figure 1. Summary of the analysis framework used in this study to simulate hydrological production potential scenarios.*

161 CC-induced RoR electricity production changes are assessed by comparing the production  
162 potential simulated for the reference period  $T_{ref}$  with that for the future periods  $T_1$ ,  $T_2$  and  $T_3$  (for all  
163 available climate model ensembles), assuming unchanged installed machinery and  
164 environmental flow requirements. Changes induced by environmental flow or by design discharge  
165 modifications are assessed by comparing the production potential for the reference period to the  
166 simulated production potential with changed environmental requirements or modified design  
167 discharge, but keeping the climate equal to that in the reference period. The analysis is  
168 complemented by an analysis of correlation between simulated changes and potential explanatory  
169 variables (Section 3.3).

## 170 2.2 Data sets

171 We use three data sets: i) the streamflow scenarios Hydro-CH2018 (BAFU 2021); ii) the Swiss  
172 HP production statistics WASTA (WASTA 2019); and iii) a georeferenced database about Swiss  
173 HP infrastructure, called HydroGIS, created by Balmer (2012). With these data sets we simulate  
174 so-called hydrological production potential scenarios (Figure 2).





175

176 *Figure 2: The flowchart used in this study to simulate hydrological production potential scenarios. The grey boxes*  
 177 *represent simulated data and models obtained from external sources, while blue boxes represent the modelling carried*  
 178 *out in this study.*

### 179 2.2.1 Hydrological scenarios Hydro-CH2018

180 The streamflow scenarios Hydro-CH2018 (BAFU 2021) are based on the most recent transient  
 181 Swiss climate change scenarios CH2018 (CH2018 2018), which are based on the EURO-  
 182 CORDEX data set (Jacob et al. 2014). The CH2018 scenarios result from climate model  
 183 simulations and subsequent statistical downscaling with the quantile mapping approach (CH2018  
 184 2018). The streamflow scenarios are based on a total of 39 CC scenarios, covering three  
 185 Representative Concentration Pathways (RCPs): RCP2.6 (concerted CC mitigation efforts),  
 186 RCP4.5 (limited CC mitigation measures), and RCP8.5 (no CC mitigation measures). For each  
 187 RCP, a varying number of climate model ensembles is available, between 1981 and 2099, which  
 188 are based on different combinations of Regional Climate Models (RCMs) and General Circulation  
 189 Models (GCMs) and thus have different spatial resolutions (Supplementary Information (SI) Table  
 190 SI1). The reference period is 1981–2010 and the future, transient climate simulations are divided  
 191 into three periods of 30 years ( $T_1$ : 2020–2049,  $T_2$ : 2045–2074,  $T_3$ : 2070–2099).

192 For the present work, daily streamflow scenarios corresponding to the 39 CC scenarios are  
 193 available from Brunner et al. (2019) (for details, see SI, Section SI1.4). The simulations used here  
 194 are based on the hydrological model PREVAH (PREcipitation streamflow EVApotranspiration

195 HRU related model; Viviroli et al. 2009), which have been used for CC impact studies in  
196 Switzerland (BAFU 2021) and have been calibrated for diverse water resource applications in  
197 Switzerland (Bernhard and Zappa 2009; Köplin et al. 2014; Speich et al. 2015) (SI, Figure SI1 &  
198 Table SI2).

199 PREVAH is a reservoir-based hydrological model that transforms spatially distributed precipitation  
200 into streamflow at selected catchment outlets, accounting explicitly for snow accumulation and  
201 snow and glacier melt. Key hydrological processes, such as evapotranspiration, infiltration into  
202 the soil, and subsequent water release via surface and subsurface runoff, are represented.  
203 Besides key spatial data derived from a digital elevation model, input consists of air temperature,  
204 precipitation, and potential evapotranspiration (computed with the Penman–Monteith equation  
205 considering wind, relative humidity, air temperature and global radiation). Compared to early  
206 applications, the model version underlying the present scenarios is improved regarding the  
207 representation of snow accumulation at high elevations (Freudiger et al. 2017) and the  
208 representation of glaciers and their length evolution (Brunner et al. 2019).

### 209 2.2.2 Hydropower production characteristics

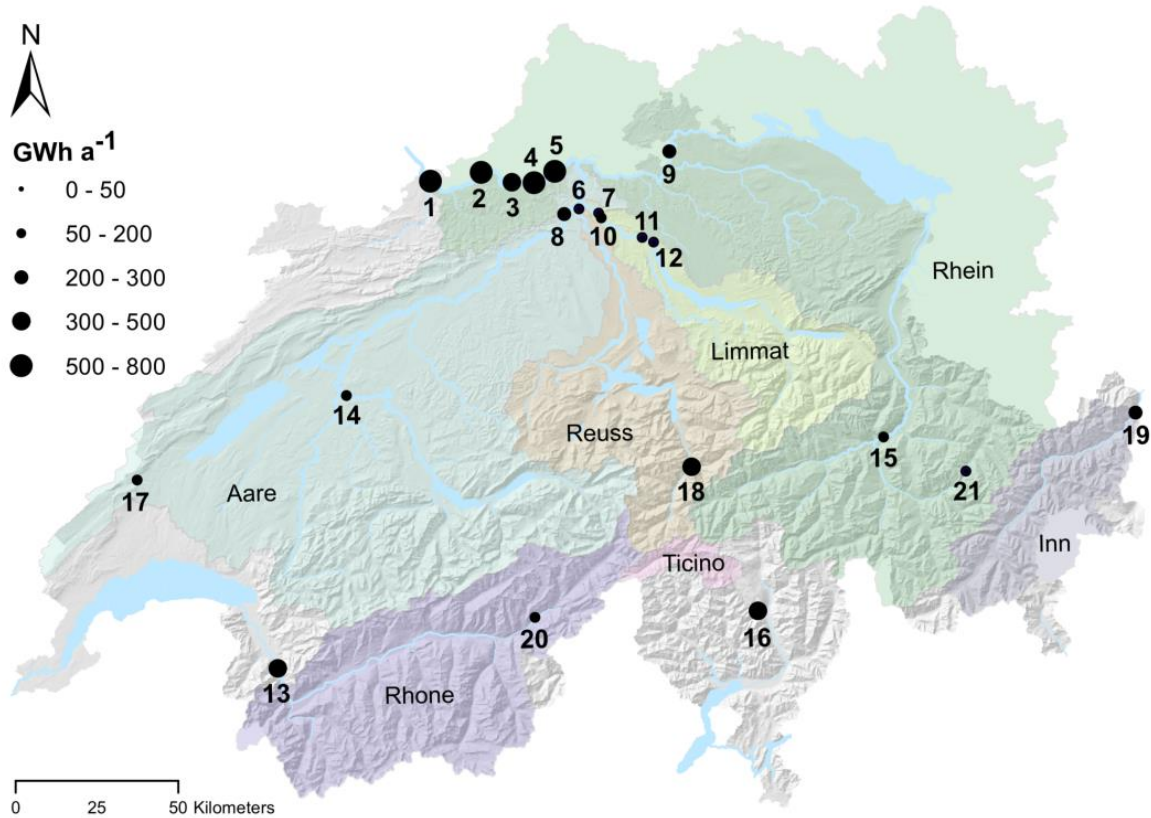
210 Two data sets are available to characterise the Swiss HP infrastructure: i) the HP plant database  
211 WASTA (WASTA 2019), which contains data on 697 powerhouses (>300 kW), including HP  
212 production type, design discharge [ $\text{m}^3 \text{s}^{-1}$ ], installed power [MW], mean annual production [GWh  
213  $\text{a}^{-1}$ ], winter production (October to March), and summer production (April to September); ii) the  
214 HydroGIS database (Balmer 2012), which contains georeferenced information on 401  
215 powerhouses and related infrastructure, including the hydrological catchment corresponding to  
216 each HP production scheme (which can be composed of several powerhouses). The data on  
217 powerhouses is directly related to WASTA (via a unique identifier). The key information extracted  
218 from HydroGIS for our work is the hydraulic head of each RoR power plant and the height  
219 difference between the water intake and the turbine axis. More details on these two data sources

220 are available in the work of Schaepli et al. (2019). It is noteworthy that the methods used to  
221 estimate the expected production that is reported in WASTA are unclear but rely on estimation  
222 models applied by the HP producers, including expected average turbine operation hours.

223 There is no database for the specific environmental flow requirements of individual Swiss RoR  
224 plants. The general rules are fixed in Swiss law (Federal Act on the Protection of Water; GSchG  
225 2011) but are adapted for each production location in the water use contracts, i.e. the so-called  
226 concessions. These requirements were obtained directly from the HP producers for the purpose  
227 of this study.

### 228 2.3 Selected case studies

229 In Switzerland, 576 RoR plants (>300 kW) produce about 21.3 TWh a<sup>-1</sup>, i.e. 31.5% of the total  
230 electricity production (BFE 2020). The largest RoR plants are located along the major streams in  
231 the so-called Plateau region of Switzerland (the low-elevation region). Similar to in other Alpine  
232 regions, there are also numerous small and medium-sized RoR plants (in terms of installed  
233 power) at higher elevations in the mountains. In this study we consider 21 RoR power plants  
234 (Figure 3). They span a wide variety of hydro-climatological regimes, but some of these RoR  
235 power plants are located along the same river to show differences between sequential plants.



236

237 *Figure 3. Location of the selected 21 RoR power plants in Switzerland. The size of the power plants corresponds to the*  
 238 *annual production in GWh a<sup>-1</sup>. The numbering (see Table 1) is arranged in ascending order according to the elevation*  
 239 *[m a.s.l.] of the power plant's water intake. The coloured areas represent the main hydrological catchment areas in*  
 240 *Switzerland.*

241 The 21 RoR power plants represent different infrastructure characteristics (in terms of installed  
 242 turbine types and power), different catchment elevations, and streamflow regimes (Table 1).  
 243 Some RoR power plants are located directly on the considered river, others divert the water, and  
 244 some additionally have a limited storage reservoir. Details of all power plants are given in the  
 245 provided data set (Wechsler 2021).

246 Table 1. The selected 21 RoR power plants of this study are ordered (Nr.) according to the elevation [m a.s.l.] of the  
 247 power plant's water intake. This table gives an overview of each power plant's name, the river on which it is located,  
 248 the area and mean elevation of the catchment contributing to the streamflow, the presence of a water diversion, the  
 249 installed power ( $P$ ), the simulated electricity production for the reference period ( $E_{ref}$ ), the power plants' design  
 250 discharge ( $Q_d$ ), and the minimum flow that has to be provided for environmental flow requirements or fish passability  
 251 ( $Q_e$ ). More details on the specific technical characteristics of each power plant are available in the provided data set  
 252 (Wechsler 2021).

Nr.	Power Plant	River	Area [km <sup>2</sup> ]	ØElevation [m a.s.l.]	Diversion [Yes/No]	$P$ [MW]	$E_{ref}$ [GWh a <sup>-1</sup> ]	$Q_d$ [m <sup>3</sup> s <sup>-1</sup> ]	$Q_e$ [m <sup>3</sup> s <sup>-1</sup> ]
1	Birsfelden	Rhein	34'981	1064	N	97.5	557.7	1500	6
2	Ryburg-S.	Rhein	34'470	1072	N	120	698.2	1460	6
3	Saeckingen	Rhein	34'277	1074	N	72	479.4	1450	2
4	Laufenburg	Rhein	34'055	1078	N	106	630.7	1370	10
5	Albbruck-D.	Rhein	33'710	1081	Y	83.8	581.4	1100	2
6	Windisch	Reuss	3'421	1249	Y	2.01	12.3	55	10
7	Aue	Limmat	2'394	1131	Y	5	26	117	14
8	Wildeggen-B.	Aare	11'640	1004	Y	49.7	289.3	400	20
9	Rheinau	Rhein	11'952	1241	Y	36	246.1	400	5
10	Wettingen	Limmat	2'394	1131	Y	24	134.7	133	1.9
11	Höngg	Limmat	2'186	1190	Y	1.3	10	50	5
12	Letten	Limmat	1'828	1222	Y	4.2	20.8	100	5
13	Lavey	Rhone	4'741	2192	Y	70	412.1	220	10
14	Mühleberg	Aare	3'168	1522	N	40	156.4	301	0
15	Reichenau	Rhein	3'210	2015	Y	18	111.8	120	4.3
16	Biaschina	Ticino	313	1913	Y	135	360.6	54	1
17	Les Clées	Orbe	299	1196	Y	30	103.3	21	0.7
18	Amsteg	Reuss	595	2167	Y	120	461.1	50	4
19	Kh. Prutz/Ried	Inn	1'941	2342	Y	86.9	411	75	7
20	Aletsch	Massa	196	2929	Y	35.3	184.8	7	0
21	Glaris	Landwasser	196	2209	Y	0.96	7.5	2.1	0.373

253  
 254 The 21 selected RoR power plants produce a total of 5.9 TWh a<sup>-1</sup>, corresponding to 36% of the  
 255 mean annual RoR production of Switzerland (2010–2019). Winter production amounts to 2.5 TWh  
 256 w<sup>-1</sup> (43% of mean winter RoR production) and summer production to 3.4 TWh s<sup>-1</sup> (31% of mean  
 257 summer RoR production). The ensemble of 21 plants includes 5 plants with a small annual  
 258 production (< 50 GWh a<sup>-1</sup>), 12 plants with an annual production between 50 and 500 GWh a<sup>-1</sup>,  
 259 and 4 large plants with an annual production > 500 GWh a<sup>-1</sup>.

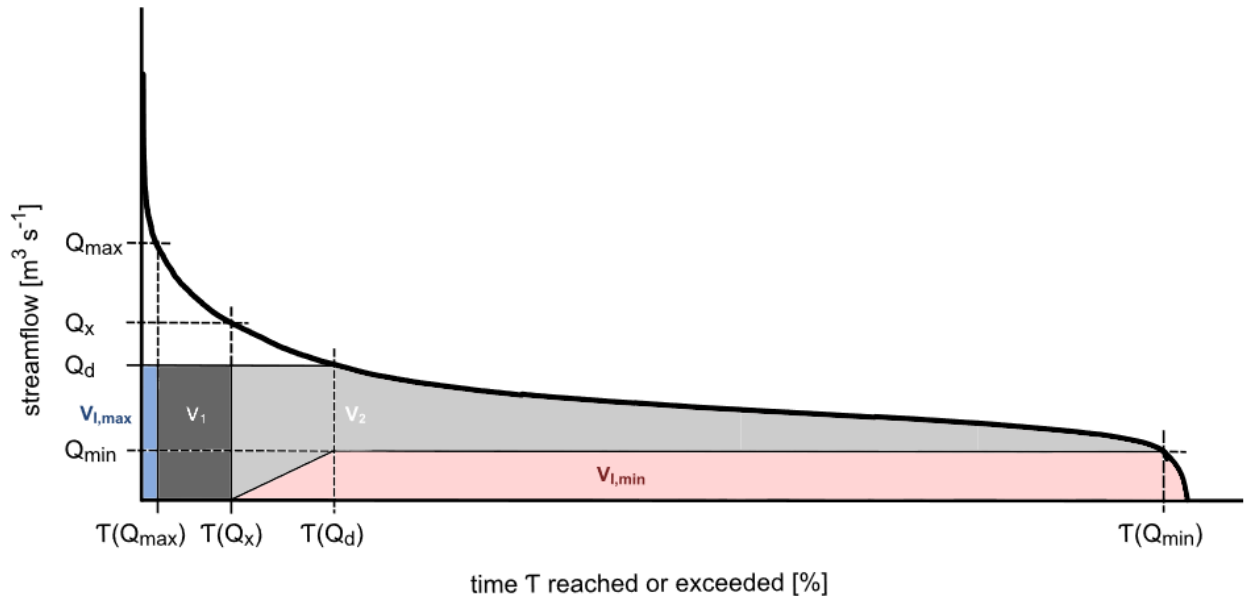
## 260 2.4 Methods

### 261 2.4.1 Quantification of usable streamflow volume for electricity production

262 The first step in the estimation of RoR production potential is the estimation of the expected  
263 available streamflow volume, which is based on the Flow Duration Curve (FDC); this is an inverse  
264 representation of the cumulative probability distribution of streamflow (Vogel and Fennessey  
265 1995) and is classically used for RoR design (Westerberg et al. 2011; Hänggi and Weingartner  
266 2012; Wagner et al. 2017; Kuriqi et al. 2019). It allows the quantification of the expected available  
267 streamflow volume for production  $V_{\text{exp}}$ , accounting for the full distribution of streamflow, for the  
268 design discharge  $Q_d$ , and for the non-usable streamflow volume  $V_{l,\text{min}}$ , e.g. because of known  
269 water abstractions for irrigation or because of environmental flow requirements, i.e. water flows  
270 reserved for ecological purposes. As illustrated in Figure 4,  $V_{\text{exp}}$  is estimated as the integral of all  
271 streamflow values  $Q(T)$  that are smaller than the design discharge  $Q_d$  (exceeding streamflow  
272 cannot be turbined) minus the volume lost to minimum flow  $V_{l,\text{min}}$  and minus additional production  
273 loss  $V_{l,\text{max}}$ .  $V_{l,\text{max}}$  results from the maximum streamflow  $Q_{\text{max}}$  during which the system still can be  
274 safely operated. Beyond  $Q_{\text{max}}$ , the production system is shut down to prevent damage, to the  
275 water intake, e.g. by driftwood. As can be seen in Figure 4,  $V_{\text{exp}}$  can thus be calculated as follows  
276 (Hänggi and Weingartner 2012):

$$277 \quad V_{\text{exp}} = V_1 + V_2 = Q_d(\tau(Q_x) - \tau(Q_{\text{max}})) + \sum_{\tau(Q_x)}^{\tau(Q_{\text{min}})} (Q_d + Q_{\text{min}}), \quad (1)$$

278 where  $T$  is the duration during which a streamflow is reached or exceeded.



279

280 *Figure 4. Illustration of the estimation of the hydrological production potential based on the Flow Duration Curve (FDC),*  
 281 *characterised by the parameters  $Q_{max}$  [ $m^3 s^{-1}$ ],  $Q_d$  [ $m^3 s^{-1}$ ] and  $Q_{min}$  [ $m^3 s^{-1}$ ].  $\tau(Q_x)$  [%] designates the duration during*  
 282 *which the streamflow reaches  $Q_d+Q_{min}$ , adapted from the work of Hänggi and Weingartner (2012).  $V_{l,max}$  and  $V_{l,min}$*   
 283 *indicate the loss due to  $Q_{max}$  or  $Q_{min}$ .*

284  $Q_d$  values are specific to the installed turbines and are available via the WASTA database.  $Q_{min}$   
 285 values must be collected from HP concessions, i.e. the plant-specific water use contracts.  $Q_{max}$   
 286 values are difficult to determine in practice because these values are not formally fixed; we ignore  
 287 them in this study, resulting in  $T(Q_{max}) = 1$  day. The resulting error can be assumed to be small.  
 288 In this study, the production estimation is based on daily streamflow values, which increases the  
 289 uncertainty, especially for RoR plants in small catchments, as they are exposed to stronger sub-  
 290 daily streamflow fluctuations than plants operating with streamflow from larger catchments. RoR  
 291 plants downstream of lakes are less affected. FDCs (i.e. streamflow distributions) are obtained  
 292 here by ranking the entire streamflow time series, available from daily simulations (Section 2.2.1).  
 293 FDCs for winter are based on the daily streamflow values for October to March, and those for  
 294 summer are based on values for April to September.

295 **2.4.2 Calculation of RoR electricity production**

296 The installed power  $P$  [MW;  $10^6$  kg  $m^2 s^{-3}$ ] of a RoR power plant is computed as:

297  $P = Q_d H \varphi \eta g,$  (2)

298 where  $H$  [m] is the hydraulic head (the difference in height between the water intake and the  
299 turbine axis),  $\varphi$  [kg m<sup>-3</sup>] is the density of water,  $\eta$  [-] is the specific efficiency of the machinery,  $g$   
300 [m s<sup>-2</sup>] is the gravitation, and  $Q_d$  [m<sup>3</sup> s<sup>-1</sup>] is the design discharge of the installed turbines.

301 The three parameters  $\varphi$ ,  $\eta$  and  $g$  can be combined into a single factor  $F$  [kg m<sup>-2</sup> s<sup>-2</sup>], a simplified  
302 overall efficiency:

303  $F = \varphi \eta g .$  (3)

304 The specific efficiency  $\eta$  of a HP plant depends on several factors, including the runner, turbine  
305 type, generator capacity, or friction loss in the penstock (Basso and Botter 2012; Yildiz and Vrugt  
306 2019). We consider  $\eta$  to be constant here, but it is in principle time-variant, depending in particular  
307 on the actual discharge through each turbine (if there are several). We make the assumption that  
308 the machinery of all RoR plants allows HP production at a relatively constant efficiency.

309 The actual value of  $F$  is unknown; it can be estimated from Equation 4 if the installed power is  
310 known and if we make the assumption that the hydraulic head  $H$  is constant (a simplification  
311 necessary here since we do not have data on actual hydraulic heads):

312  $F = \frac{P}{Q_d H} .$  (4)

313 The corresponding specific efficiency  $\eta$  is thus:

314  $\eta = \frac{P}{Q_d H \varphi g} ,$  (5)

315 which theoretically is between 0.7 and 0.9 (Laufer et al. 2004).  $\eta$  [-] is usually somewhat higher  
316 for RoR power plants than for storage power plants, because the penstocks are mostly shorter  
317 and thus the loss due to friction is smaller.



318 The actual RoR electricity production  $E'(t)$  [MWh] at a given time step  $t$  is obtained by replacing  
319 the design discharge  $Q_d$  by actual discharge  $Q(t)$  in Equation 2 and by multiplying by the turbine  
320 operation time  $T_{\text{Turb}}$  (=1 day):

$$321 \quad E'(t) = Q(t) H F \tau_{\text{Turb}}(t) = V(t) H F. \quad (6)$$

322 The ' in  $E'(t)$  highlights here the instantaneous production and differentiates it from the expected  
323 production  $E$ . This expected production  $E$  is obtained by replacing  $V(t)$  in the above equation by  
324  $V_{\text{exp}}$  from Equation 1:

$$325 \quad E = V_{\text{exp}} H F. \quad (7)$$

326 In this formulation, we assume that the turbines are fully operational whenever there is water to  
327 produce.

328 The production loss  $E_e$  arising from an imposed minimum environmental flow (Figure 4) is  
329 calculated as:

$$330 \quad E_e = V_{l,\text{min}} H F. \quad (8)$$

331 We also quantify an optimised annual production,  $Q_{\text{opt}}$  [ $\text{m}^3 \text{s}^{-1}$ ], that could be obtained by  
332 increasing the design discharge (which is theoretical because it would require replacing the  
333 turbines). In fact, most of the Swiss RoR power plants were built in the period 1920–1970 with  
334 the technology and requirements of the time. The design of the earliest RoR power plants was  
335 based on little streamflow data and sometimes based on local electricity need considerations (e.g.  
336 of a nearby factory) rather than from an optimal streamflow use perspective. In the meantime,  
337 production technology has become more efficient, and actual streamflow variability can be  
338 assessed based on streamflow or electricity production records. Accordingly, some RoR plants  
339 might today show a considerable optimisation potential of the design discharge in relation to the  
340 actual streamflow regime (Yildiz and Vrugt 2019). The theoretical optimised design discharge

341 considered here corresponds to streamflow that is exceeded 20% of the time, as a rough  
342 benchmark for new power plants. We thus obtain a new  $V_{exp,opt}$  by replacing  $Q_d$  by  $Q_{opt} = Q_{20}$  in  
343 Equation 1.

$$344 \quad E_{opt} = V_{exp,opt} H F. \quad (9)$$

345 The data required to estimate  $E$ ,  $E_e$  and  $E_{opt}$  are obtained as follows: installed power  $P$  and design  
346 discharge  $Q_d$  are from WASTA (Section 2.2.2), the hydraulic head  $H$  [m] is from the HydroGIS  
347 data set (Section 2.2.2),  $Q_{min}$  (underlying  $V_{exp}$ ) is from detailed personal enquiry, and streamflow  
348 (underlying  $V_{exp}$ ) is from hydrological simulations (Section 2.2.1). WASTA also provides estimates  
349 of expected annual production. This data is used to optimise  $\eta$  and thus  $F$  in cases where there  
350 are any major discrepancies (see full data set in the Supplementary Data; Wechsler 2021).

### 351 2.4.3 Uncertainty quantification

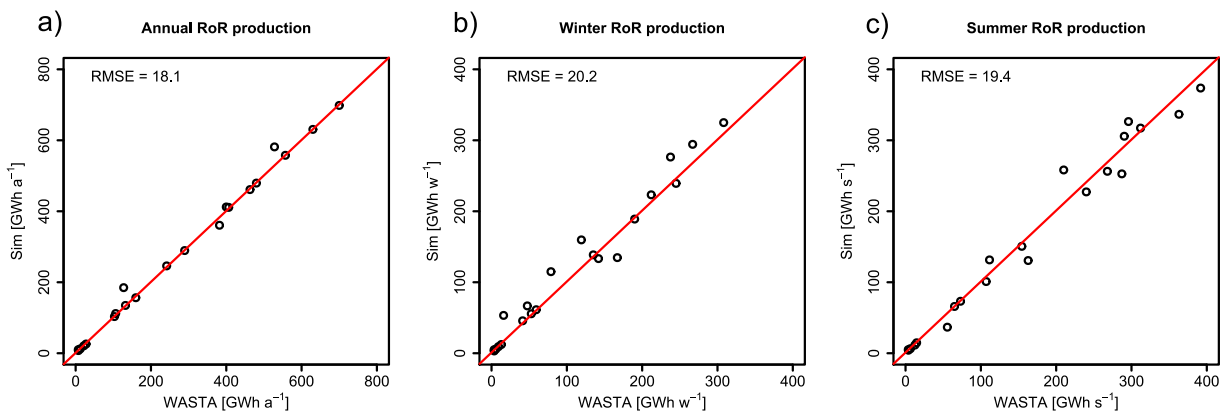
352 Uncertainties inherent in the hydroclimatic scenarios are handled in this study via the use of  
353 streamflow ensemble simulations resulting from the simulation framework (see Section 2.2.1). To  
354 gain further insights into uncertainties related to simulated production, we compare the collected  
355 production data (WASTA, Section 2.2.2) to the simulated RoR production based on the climate  
356 model ensembles (Section 3.1). The uncertainties in this simulated production result from our  
357 simplified assumptions of constant hydraulic head  $H$  [m] and of constant overall efficiency  $F$  [ $\text{kg}$   
358  $\text{m}^{-2} \text{s}^{-2}$ ], which both depend on actual streamflow conditions. To more accurately account for the  
359 impacts of varying hydraulic head  $H$  [m] and of varying streamflow on overall efficiency  $F$  [ $\text{kg}$   $\text{m}^{-2}$   
360  $\text{s}^{-2}$ ], operational RoR power plant data would be needed.

## 361 3 Results

### 362 3.1 Validation of the current RoR electricity production

363 In a first step, the reference period simulations are compared to the expected production listed in  
364 the HP infrastructure database (WASTA, Section 2.2.2), on the annual and seasonal level. The

365 estimated production considers environmental flow requirements and infrastructure  
 366 characteristics for the 21 RoR power plants in this study. The estimated total mean annual  
 367 production of all 21 RoR power plants during the reference period (5895.2 GWh a<sup>-1</sup>) agrees well  
 368 with WASTA data (5782.5 GWh a<sup>-1</sup>); winter production (October to March) tends to be slightly  
 369 overestimated ( $\Delta +192.7$  GWh w<sup>-1</sup>) and summer production (April to September) tends to be  
 370 slightly underestimated ( $\Delta -43.3$  GWh s<sup>-1</sup>; Figure 5). Given these good validation results, we do  
 371 not further analyse production uncertainties arising from the simplified production model. Details  
 372 on streamflow validation are available in the Supplementary Information (Table SI2, Figure SI2).



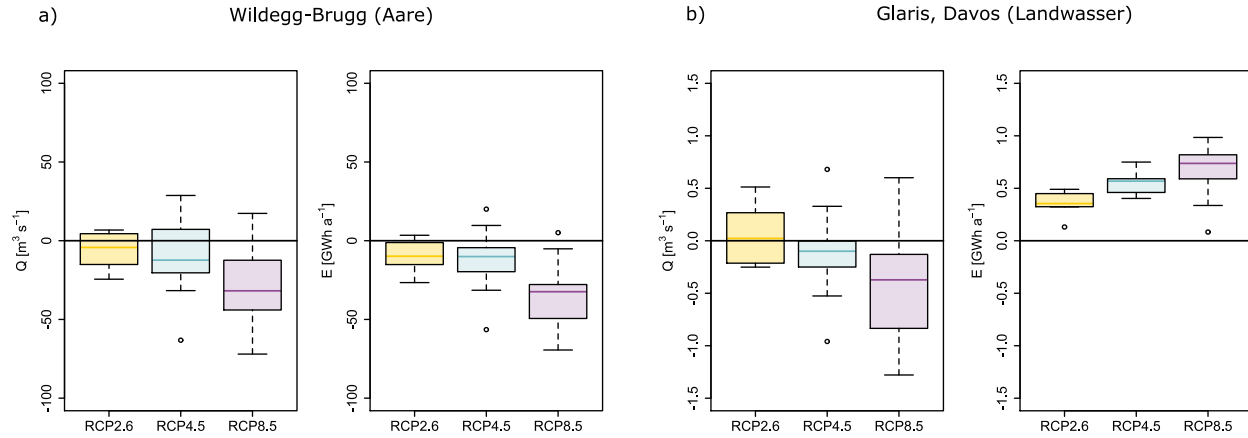
373

374 *Figure 5. Comparison of the mean simulated production with production reported in the WASTA database for the 21*  
 375 *RoR plants: a) annual production, b) winter production (October to March), and c) summer production (April to*  
 376 *September).*

## 377 3.2 Change in RoR electricity production

### 378 3.2.1 Case study of two RoR power plants

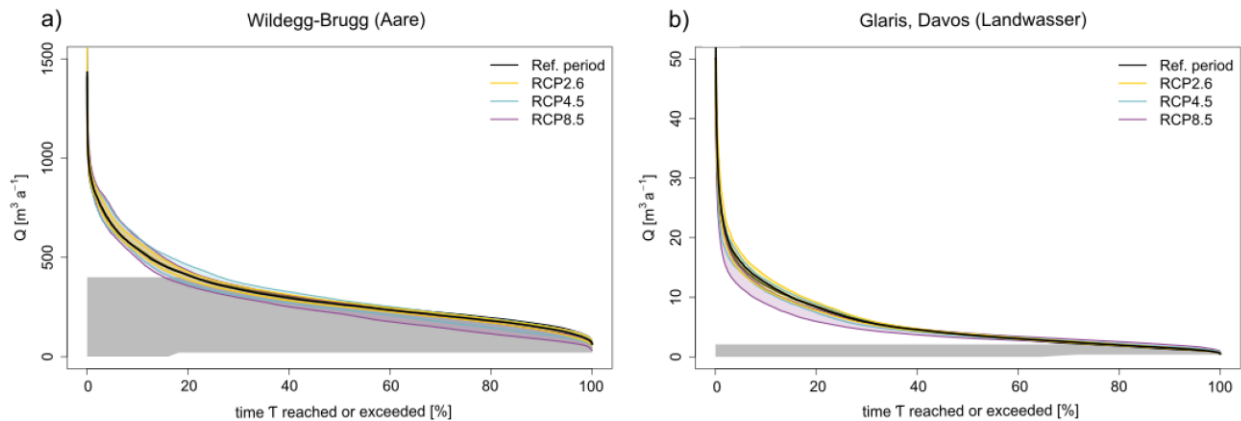
379 The impacts of CC, environmental flow requirements, and optimised design discharge on RoR  
 380 electricity production are calculated with the FDC for each of the 21 RoR power plants. We  
 381 illustrate here the detailed results for two representative plants, the Wildegg-Brugg power plant  
 382 and the Glaris, Davos power plant. Full results are available in the Supplementary Data (Wechsler  
 383 2021). The Wildegg-Brugg power plant shows both a decrease in annual streamflow and a  
 384 reduction in annual production by the end of the century (Figure 6a); the Glaris, Davos power  
 385 plant shows only minor changes in streamflow, but an increase in annual production (Figure 6b).



386

387 *Figure 6. Simulated changes in the mean annual streamflow (Q) and mean electricity production (E) by the end of the*  
 388 *century (2070–2099) at a) the Wildegg-Brugg power plant and b) the Glaris, Davos power plant. The black line indicates*  
 389 *the median value of the reference period (1981–2010). The yellow (RCP2.6), blue (RCP4.5) and purple (RCP8.5)*  
 390 *boxplots represent the range of the different model ensembles based on the three emissions scenarios.*

391 This difference is caused by differences in the infrastructure characteristics of the power plants.  
 392 If the changes in streamflow are in the range that can be used for RoR electricity production, this  
 393 has an immediate influence. At the Glaris, Davos power plant, the streamflow increases in the  
 394 low water range, which has a positive impact on production (Figure 7).



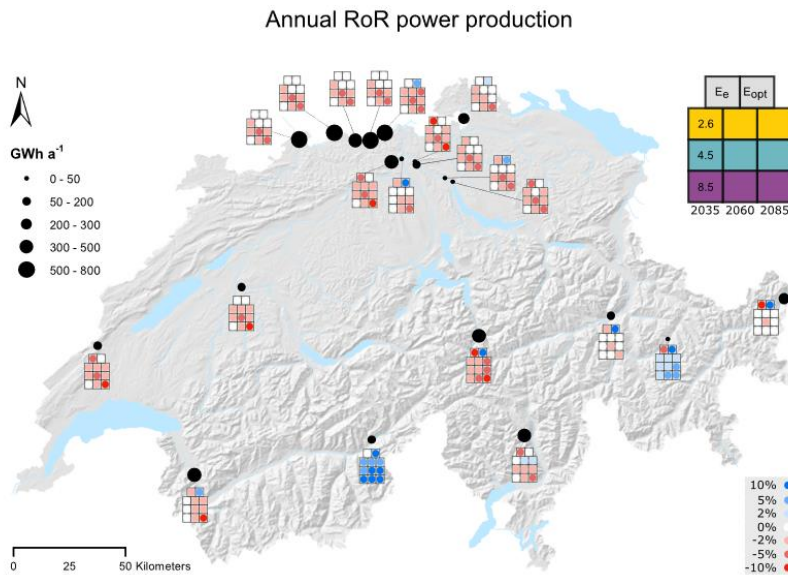
395

396 *Figure 7. Flow Duration Curves (FDCs) for the power plants a) Wildegg-Brugg and b) Glaris, Davos. The black line*  
 397 *represents the reference period (1981–2010), the grey shaded area represents the expected available streamflow*  
 398 *( $V_{exp}$ ), and the areas bounded by yellow (RCP2.6), blue (RCP4.5) and purple (RCP8.5) curves represent the range of*  
 399 *FDCs for the projected model ensembles based on the three emissions scenarios for the end of the century.*

400 The production loss due to environmental flow requirements ( $E_e$ ) is estimated at 17.5 GWh a<sup>-1</sup>,  
401 i.e. -6% of the annual production, at the Wildegg-Brugg RoR power plant and 0.5 GWh a<sup>-1</sup>, i.e. -  
402 6%, at the Glaris, Davos plant. The potential for increasing production by optimising the design  
403 discharge ( $E_{opt}$ ), so that it corresponds to streamflow that is exceeded 20% of the time, amounts  
404 to 2.5 GWh a<sup>-1</sup>, i.e. 1% of the annual production, at the Wildegg-Brugg plant and 9.8 GWh a<sup>-1</sup>, i.e.  
405 128%, at the Glaris, Davos plant (see Supplementary Data; Wechsler 2021).

### 406 3.2.2 Spatial analysis of 21 RoR power plants

407 Considering all 21 RoR power plants, the future mean annual production is predicted to decrease  
408 slightly over the century under the given CC projections (Table 2). Exceptions are the high-  
409 elevation power plants, which are strongly influenced by snow- and ice-melt processes (Figure  
410 8). The total production loss due to environmental flow requirements ( $E_e$ ) for the 21 RoR power  
411 plants is estimated at 207 GWh a<sup>-1</sup>, i.e. 3.5% of the annual production (see Supplementary Data;  
412 Wechsler 2021). The largest RoR power plants along the Rhine show little loss, while small and  
413 medium-sized power plants with diversions are most affected. The potential for increasing  
414 production by optimising the design discharge ( $E_{opt}$ ) amounts to 467 GWh a<sup>-1</sup>, i.e. 8% of the annual  
415 production. The largest increase potential is related to small and medium-sized power plants in  
416 the Alpine region (Figure 8).



417

418 *Figure 8. Simulated changes in production at the 21 RoR power plants; the size of the dots (power plants) represents*  
 419 *the annual production in GWh a<sup>-1</sup>. The coloured dots in the grids represent the loss due to environmental flow*  
 420 *requirements ( $E_e$ ), the increase potential resulting from optimisation of the design discharge ( $E_{opt}$ ), and the climate*  
 421 *change impact for the periods 2035 (near future, 2020–2049), 2060 (mid-century, 2045–2074) and 2085 (end of*  
 422 *century, 2070–2099) under the three emissions scenarios RCP2.6 (yellow), RCP4.5 (blue), and RCP8.5 (purple).*

423 The annual changes in production due to CC range from 0% to -7% (Table 2). An annual loss of  
 424 7% corresponds to the electricity consumption of around 82,500 households in Switzerland  
 425 (~5000 kWh a<sup>-1</sup> per household). The projected decrease is more pronounced for later time periods  
 426 and in the absence of CC mitigation measures. The CC-induced decrease in production is of a  
 427 similar magnitude as the production loss due to environmental flow requirements ( $E_e$  -3.5%) and  
 428 as the increase potential resulting from optimisation of the design discharge ( $E_{opt}$  +8%).

429 *Table 2. Simulated change in annual RoR electricity production for the periods  $T_1$  (2020–2049),  $T_2$  (2045–2074), and*  
 430  *$T_3$  (2070–2099) under the emissions scenarios RCP2.6, RCP4.5 and RCP8.5.*

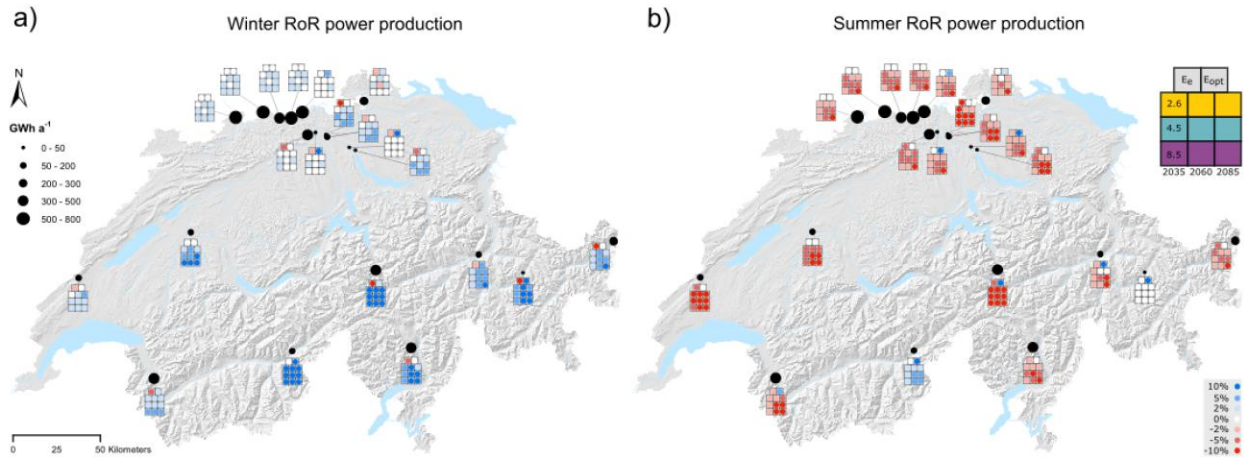
Annual	$T_1$	$T_2$	$T_3$
RCP2.6	-2%	-1%	-2%
RCP4.5	-1%	-5%	-2%
RCP8.5	0%	-3%	-7%

431

### 432 3.2.3 Overall change in seasonal RoR electricity production

433 Future winter (October to March) mean RoR electricity production is predicted to increase over  
434 the century (Figure 9). The increases are most pronounced at high elevations, where the shift  
435 from solid to more liquid precipitation increases the streamflow during winter because less water  
436 is stored in the snowpack. On the other hand, at -4.5% ( $E_e$  115 GWh  $w^{-1}$ ), the production loss due  
437 to environmental flow requirements in the winter half-year are slightly greater than the annual  
438 average. The optimisation of the design discharge can cause an increase in production by 2.5%  
439 ( $E_{opt}$  60 GWh  $w^{-1}$ ) in the winter half-year because streamflow in winter is usually below the design  
440 discharge and thus full capacity is not reached. The winter changes in RoR production due to CC  
441 range from +2% to +9% (Table 3a). The projected increase becomes more pronounced over time  
442 and without CC mitigation measures (RCP8.5). The CC-induced increase is of a similar  
443 magnitude as the production loss due to environmental flow requirements ( $E_e$  -4.5%) and the  
444 increase potential due to the optimisation of design discharge ( $E_{opt}$  2.5%). However, the projected  
445 increase in winter production does not outweigh the negative change in annual production, as  
446 winter production only accounts for 43% of the total annual production.

447 In summer (April to September), RoR production declines under CC (Figure 9b). The absence of  
448 CC mitigation measures and the time period make a large difference. The loss due to  
449 environmental flow requirements is -2.5% ( $E_e$  91 GWh  $s^{-1}$ ) and therefore less during the summer.  
450 Optimising the design discharge results in a production increase by 12% ( $E_{opt}$  404 GWh  $s^{-1}$ ). The  
451 increase potential tends to lie more at high elevations. The changes in summer RoR production  
452 due to CC range from -2% to -21% (Table 3b). The projected decrease is more pronounced in  
453 later time periods and when CC mitigation measures are absent. The CC-induced decrease in  
454 production during summer is therefore larger than the production loss due to environmental flow  
455 requirements and the increase potential due to optimisation of the design discharge.



456

457 *Figure 9. Same as Figure 8 but for a) winter (October to March) and b) summer (April to September).*

458

459 *Table 3. Simulated change in a) winter (October to March) and b) summer (April to September) RoR electricity*  
 460 *production for the periods  $T_1$  (2020–2049),  $T_2$  (2045–2074), and  $T_3$  (2070–2099) under the emissions scenarios*  
 461 *RCP2.6, RCP4.5 and RCP8.5.*

a) Winter	$T_1$	$T_2$	$T_3$	b) Summer	$T_1$	$T_2$	$T_3$
RCP2.6	+2%	+5%	+4%	RCP2.6	-5%	-4%	-2%
RCP4.5	+5%	+4%	+7%	RCP4.5	-6%	-11%	-9%
RCP8.5	+5%	+7%	+9%	RCP8.5	-5%	-10%	-22%

462

### 463 3.2.4 Synthesis of the simulated electricity production projections

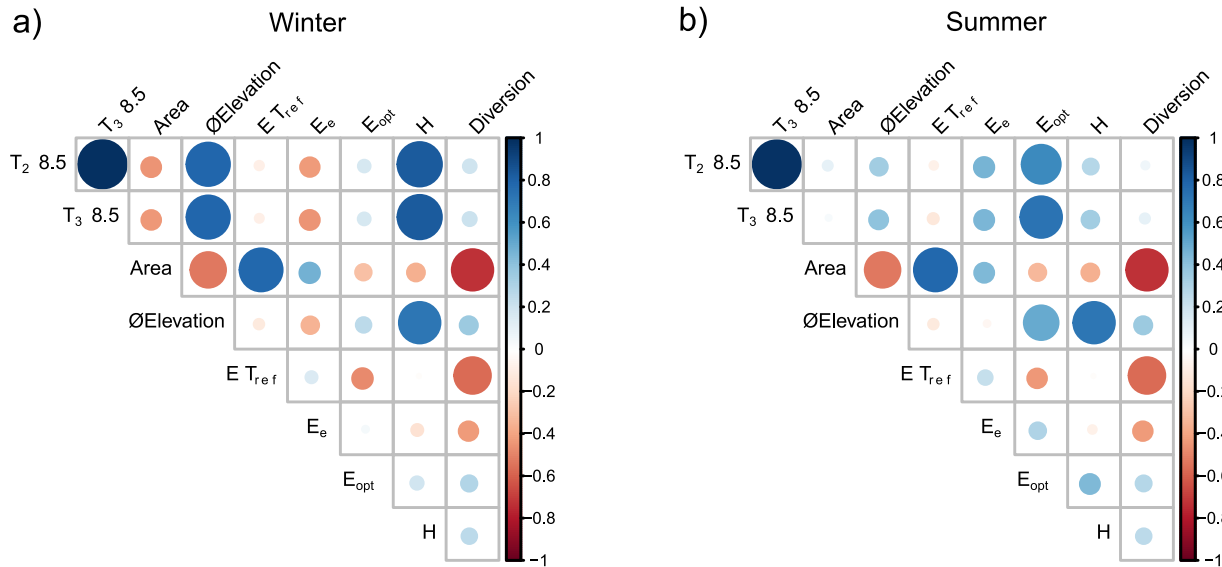
464 The simulated CC impacts are, from mid-century onwards, similar to the estimated annual  
 465 production loss due to environmental flow requirements, which equals, on average, 3.5% of the  
 466 simulated production during the reference period (1981–2010). For 11 of the 21 plants, design  
 467 discharge optimisation would lead to a production increase of between 1% and 149% (average  
 468 increase of 45% for these 11 plants; total increase corresponds to 8% of the current production).  
 469 For six of these 11 plants, this could compensate the loss due to environmental flow requirements.  
 470 For five of them, design discharge optimisation would compensate expected CC-induced loss  
 471 under the most extreme scenario (RCP8.5) by the end of the century.



### 472 3.3 Key variables explaining the change in RoR electricity production

473 To gain further insight into what might explain the observed changes in RoR production, we  
474 analyse the correlations (linear and rank correlations) between the simulated production changes  
475 and i) underlying streamflow changes due to CC and ii) technical plant characteristics. The  
476 impacts on production that are related to the different scenarios and time periods are strongly  
477 correlated to each other (lowest linear correlation of 0.78); accordingly, we only present the results  
478 for RCP8.5 below. The corresponding data for RCP2.6 and RCP4.5 are available in the  
479 Supplementary Data (Wechsler 2021).

480 A correlation analysis with selected power plant characteristics (Figure 10) reveals that mean  
481 catchment elevation [m a.s.l.] is an important variable influencing future changes in RoR electricity  
482 production. There is a distinct positive correlation ( $>0.68$ ) between the mean catchment elevation  
483 ( $\bar{z}$  elevation) and the CC-induced production changes (at  $T_2$  and  $T_3$  for the emissions scenario  
484 RCP8.5). The plants at the highest elevations show a production increase under all emissions  
485 scenarios and for all time periods. With one exception (see full results table in Supplementary  
486 Data; Wechsler 2021), such positive production changes are only simulated for power plants with  
487 a mean elevation higher than 1900 m a.s.l. This elevation dependence needs to be considered in  
488 relation to the actual production, which is the highest for the large low-elevation HP plants that  
489 turbine large streamflow volumes and for which the mean annual production will systematically  
490 decrease. Furthermore, a seasonal analysis (Figure 9) shows that the mean catchment elevation  
491 correlates more strongly with the changes in winter production ( $>0.79$ ) than with the changes in  
492 summer production ( $>0.35$ ).



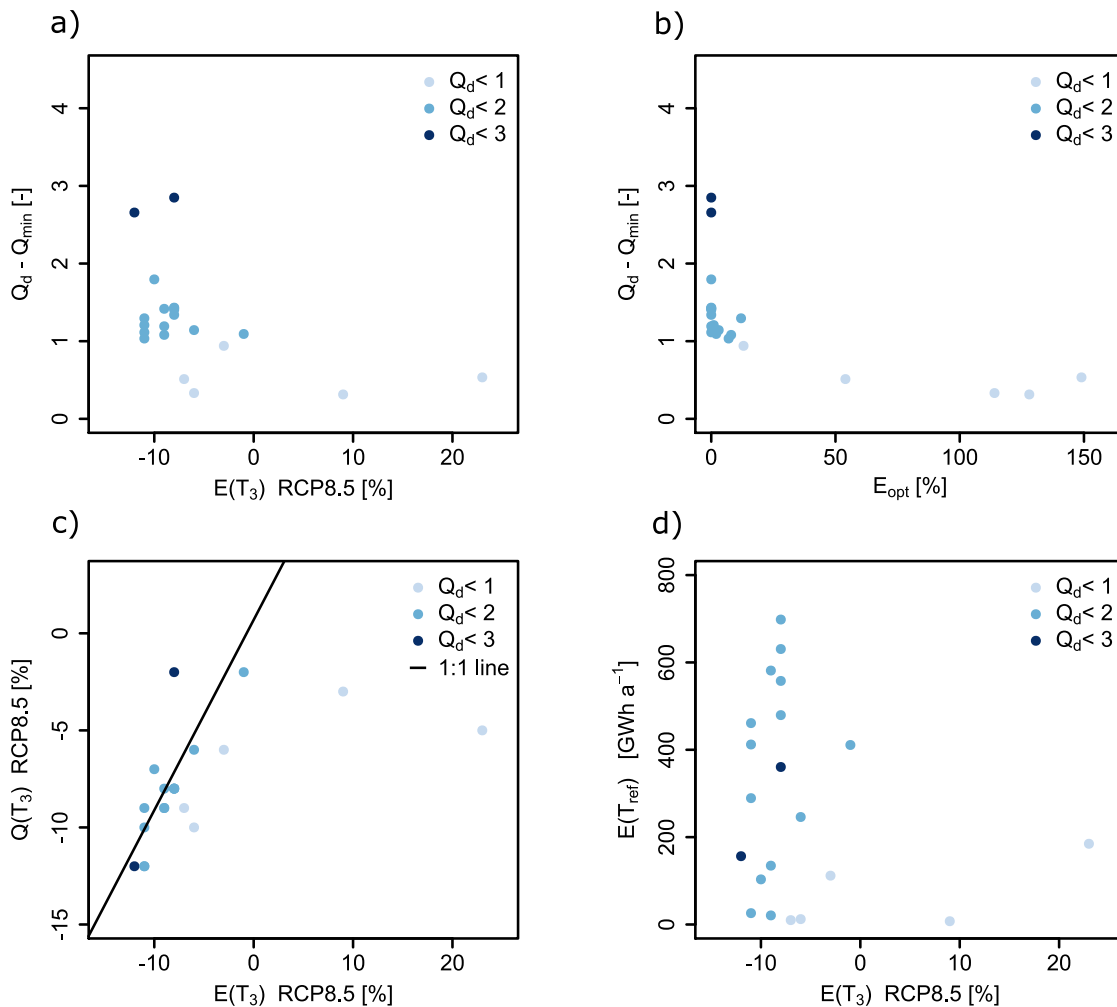
493

494 *Figure 10. Correlation matrix for a) winter (October to March) and b) summer (April to September) RoR electricity*  
 495 *production: the simulated production changes under the emissions scenario RCP8.5 for: the two future periods  $T_2$*   
 496 *(2060) [%] and  $T_3$  (2085) [%], the catchment area [ $km^2$ ], the mean elevation of the catchment [m a.s.l.], the mean annual*  
 497 *production during the reference period ( $E T_{ref}$  [ $GWh a^{-1}$ ]), the loss due to environmental flow requirements ( $E_e$  [%]), the*  
 498 *increase potential resulting from optimisation of the design discharge ( $E_{opt}$  [%]), the hydraulic head  $H$  [m], and*  
 499 *streamflow diversion (Diversion [Yes/No]). Blue dots indicate a positive correlation and red dots indicate a negative*  
 500 *correlation, with larger dots indicating stronger correlations.*

501 This relationship between mean catchment elevation and CC-induced changes in production  
 502 potentially results from several factors related to: i) infrastructure characteristics: higher-elevation  
 503 plants have higher hydraulic heads and smaller catchments, i.e. less average streamflow and  
 504 smaller design discharge; and ii) hydrological regime: higher-elevation plants have a regime with  
 505 marked differences between summer and winter streamflow.

506 There is additionally a marked negative rank correlation (-0.6) between annual production  
 507 changes and the range of usable streamflow volume, i.e. the difference between normalised (by  
 508 the mean streamflow) design discharge and normalised environmental flow; the plants for which  
 509 this range is very large are most likely to see a production decrease (Figure 11a). This is explained  
 510 by the fact that if this usable streamflow volume range is large, the projected streamflow  
 511 decreases will more directly translate to production decreases.

512 We do not detect any further relationships in terms of linear correlations or Spearman rank  
 513 correlations between production changes and other infrastructure characteristics, in particular the  
 514 ratio between  $Q_{20}$  and the design discharge, a proxy for how much of the streamflow is currently  
 515 used for production.



516

517 *Figure 11. Negative Spearman correlations a) between future annual electricity production (E) changes by time period*  
 518  *$T_3$  (2070–2099) under emissions scenario RCP8.5 and the range of usable streamflow volume (the difference between*  
 519 *normalised design discharge  $Q_d$  and normalised environmental flow  $Q_{min}$ ) and b) between the production increase*  
 520 *potential ( $E_{opt}$ ) and the range of usable streamflow volume. Comparisons of c) streamflow changes (Q) and production*  
 521 *changes (E) by  $T_3$  under RCP8.5, indicating also a linear 1:1 line, and d) annual production during the reference period*  
 522 *( $E T_{ref}$ ) and projected production (E) changes by  $T_3$  under RCP8.5. The colours of the dots represent the normalised*  
 523 *(by the mean streamflow) design discharge ( $Q_d$ ) of the 21 run-of-river power plants, with darker shades indicating higher*  
 524  *$Q_d$  values.*

525 There is no significant linear or rank correlation between the annual production loss due to  
526 environmental flow requirements ( $E_e$ ) and the CC-induced production changes or between  
527 production increase potential ( $E_{opt}$ ) and CC impacts. However, the plants that have the greatest  
528 optimisation potential are those that currently have a small usable streamflow range (small  
529 difference between normalised  $Q_d$  and normalised environmental flow  $Q_{min}$ ) (Figure 11b).

530 Changes in streamflow do not show a linear relationship with CC-induced changes in production  
531 (Figure 11c). Production changes are instead modulated by the currently used range of  
532 streamflow (which is influenced by environmental flow requirements and design discharge) and  
533 by how this range is affected by CC.

534 The RoR power plants with small design discharge ( $Q_d < 1$ ) show a non-linear relationship between  
535 streamflow changes and production changes, with two of them showing an increase in production  
536 despite decreasing streamflow (Figure 11c). The power plants with a small  $Q_d$  are predominantly  
537 small or medium-sized (Figure 11d).

538 At the seasonal scale, we see some additional patterns: In winter, loss due to environmental flow  
539 requirements are more likely to occur for higher-elevation plants with streamflow diversion, where  
540 a stronger increase in winter production is predicted (Figure 9 and results table in Supplementary  
541 Data; Wechsler 2021). The summer half-year is less affected by production reductions resulting  
542 from environmental flow requirements, whereas optimising the design discharge ( $E_{opt}$ ) is more  
543 important in summer and mainly affects the power plants at higher elevations (Figure 9 and results  
544 table in Supplementary Data; Wechsler 2021).

## 545 4 Discussion

546 In this study, we estimate the extent to which RoR electricity production will be affected by climate  
547 change (CC). Due to its steep gradients, the Alps are particularly affected by CC, which

548 particularly affects RoR power plants because they have no or limited storage. Because the study  
549 area is limited to Switzerland, the institutional framework conditions are comparable across all the  
550 studied power plants, which is especially important for the analysis of environmental flow  
551 requirements. The optimisation of the design discharge is included here to shed additional light  
552 on the implications of anticipated CC impacts. Optimisation of the design discharge can only be  
553 achieved in combination with replacement of the turbine or the runner.

554 The present study confirms the CC trends observed in previous streamflow studies in the Alps  
555 (Hänggi and Weingartner 2012; Wagner et al. 2017; Totschnig et al. 2017; Savelsberg et al. 2018;  
556 François et al. 2018; Schaepli et al. 2019), i.e. slightly decreased annual production but increased  
557 production in winter, the most critical period for electricity demand matching. The transient  
558 projections presented here include mean annual and seasonal production over 30 years, but they  
559 do not address interannual changes. In contrast to the study by Savelsberg et al. (2018), who  
560 compared individual years with future periods, we compare the future periods with the entire  
561 reference period ( $T_{ref}$ : 1981–2010); as a result, we show here a decrease in RoR annual  
562 production by up to 7%, which is in contradiction to the predicted increase of 4% in the Swiss  
563 mean annual RoR production by Savelsberg et al. (2018).

564 The novelty of our study, compared to previous simplified models (Wagner et al. 2017), is the  
565 consideration of both the legal framework and the infrastructure characteristics of the power  
566 plants. Even if the CC-induced decreases in annual production are similar to those reported in  
567 studies with simpler RoR models (Wagner et al. 2017; Totschnig et al. 2017), our joint analysis of  
568 the three variables CC, environmental flow requirements, and optimisation of the design  
569 discharge allows – for the first time – a comparison of the orders of magnitude of these changes  
570 that will inevitably arise in the coming decades. The analysis of the interplay of environmental flow  
571 requirements and design discharge also shows that a change in streamflow does not mean a  
572 linear change in production (François et al. 2014, Mohor et al. 2015) and, taken a step further,

573 that a change in production does not mean a linear change in financial revenue (Ranzani et al.  
574 2018; Savelsberg et al. 2018; Cassagnole et al. 2020).

575 The available national-scale data sets (WASTA 2019; Balmer 2012) provide a solid basis to  
576 estimate the impacts based on the specific infrastructure characteristics of RoR power plants.  
577 Although influencing variables, such as hydraulic head ( $H$ ) and factor of efficiency ( $F$ ), are  
578 simplified, the consideration of plant-specific parameters nevertheless identifies key variables that  
579 are relevant for production impacts. The real efficiency of a power plant varies in time with  
580 streamflow, which influences the hydraulic head; both head and streamflow influence the  
581 operating point of the turbines and the water-to-electricity conversion efficiency. Due to the lack  
582 of operational RoR power plant data, we could not consider further the varying efficiency as done  
583 in technical HP studies (Skjelbred and Kong 2019; Quaranta et al. 2022). The added value of  
584 considering the specific infrastructure characteristics, compared to previous studies, is that the  
585 loss due to the environmental flow requirements and the technical increase potential resulting  
586 from an adjusted design discharge can be analysed.

587 Production reductions due to environmental flow requirements are greater in the winter half-year  
588 and tend to affect small and medium-sized power plants at higher elevations and with diversions.  
589 The loss due to environmental flow requirements ( $E_e$ ) do not show a correlation with CC  
590 production loss, despite the fact that  $E_e$  influences the usable streamflow volume; this is because  
591 environmental flow affects all plants similarly, whereas design discharge is plant specific. RoR  
592 power plants with a relatively small design discharge ( $Q_d$ ) are less affected by CC.

593 The production increase potential related to a systematic application of a more optimal design  
594 discharge shows a large spread between the studied HP plants. This stems from the considerable  
595 differences in the design and construction standards underlying the different plants. The selected  
596 optimised design discharge, corresponding to streamflow that is exceeded 20% of the time, does  
597 not represent an agreed-upon reference design value, but rather shows the potentially important

598 HP production gain that is related to technical choices. It is noteworthy that the optimisation of the  
599 design discharge corresponds only to a single factor in terms of technical efficiency increase and  
600 ultimately in terms of production increase. Future CC impact studies on RoR electricity production  
601 should focus on further technical optimisation potential, considering operational RoR power plant  
602 data.

603 Finally, we acknowledge that we include only a single environmental aspect of HP production,  
604 which is the minimum flow. With regard to the future of RoR electricity production, many other  
605 environmental aspects are relevant, including sediment or fish connectivity and the problem of  
606 streamflow variability for ecosystem function (Gorla and Perona 2013; Gabbud and Lane 2016;  
607 Kuriqi et al. 2019; 2021; Carolli et al. 2022). Future work could potentially address such aspects,  
608 which are already part of the Swiss (GSchG 2009) and European legislation (Kaika 2003), to  
609 integrate the water-energy-ecosystem nexus into regional development processes (Temel et al.  
610 2023). This could ultimately contribute to the balancing of socio-economic and environmental  
611 interests in RoR development. Switzerland has a legal framework regarding environmental flow  
612 that differs from Europe. Europe's Water Framework Directive (WFD) defines more the principles  
613 for determining the environmental flow requirements, which should be considered in the  
614 respective national frameworks. The WFD not only foresees a minimum flow, but also states that  
615 the flow regime should allow a good ecological river status (EU 2015). In the Swiss legal  
616 framework, the streamflow value  $Q_{347}$  (95% percentile) serves as a reference for the determination  
617 of the minimum flow (GSchG 2011). These differences in the legal frameworks need to be  
618 considered before transferring results to other settings.

## 619 5 Conclusions

620 Our study of 21 hydropower plants represents one of the first comprehensive analyses of climate  
621 change (CC) impacts on Run-of-River (RoR) electricity production in an Alpine context. The

622 simulated CC impacts result in a minor change of about -2% to -7% in mean annual production  
623 by the end of the century. The simulated production changes show a clear positive correlation  
624 with elevation; some RoR power plants with high-elevation catchments (i.e. fed by snow and  
625 glacier melt) show an increase in annual production, while plants with a mean catchment elevation  
626 below 1900 m a.s.l. show a decrease in production. The RoR production changes for three future  
627 time periods under three emissions scenarios indicate an intensifying loss over time and without  
628 CC mitigation measures.

629 The seasonal analysis shows that the overall decrease in annual production results from a general  
630 increase of winter production (+4% to +9%) and a decrease of summer production (-2% to -22%).  
631 The simulated annual CC impacts on production are, from mid-century onwards, similar to the  
632 estimated annual production loss due to environmental flow requirements, which equals, on  
633 average, 3.5% of the simulated production during the reference period (1981-2010). Design  
634 discharge optimisation would lead to a production increase for 11 of the 21 plants and thereby  
635 compensate production loss from CC impacts for about half of those plants under all scenarios;  
636 the optimisation can, however, compensate the loss due to environmental flow for 6 plants only.

637 The key results from this study can be summarised as follows:

- 638 • Winter RoR production, which is the most critical period for electricity demand matching,  
639 will increase under the future climate; the production increase potential by optimising the  
640 design discharge is limited during winter and is about seven times smaller than in summer.
- 641 • CC-induced future RoR production is not linearly related to the projected CC-induced  
642 changes in streamflow; production changes rather depend on the currently used range of  
643 streamflow (modulated by environmental streamflow requirements and design discharge)  
644 and by how this range is affected by CC. If the usable streamflow volume range is large,  
645 the changes in streamflow will more directly translate to production changes.



646 • CC impacts, as well as production potentials, should be interpreted in light of  
647 environmental flow impacts, which in turn depend on local needs and infrastructure  
648 characteristics, in particular the presence of diversions.

649 These results might be of key importance for decision making in the field of renewable electricity  
650 production. Further work could focus on ecological impacts of changing environmental flow  
651 requirements and technical optimisation potentials. Future studies could additionally address how  
652 to deal with the two contrasting goals of energy transition, which are aiming for more renewable  
653 electricity production while reducing negative impacts on freshwater ecosystems.

#### 654 **Acknowledgements**

655 The authors gratefully acknowledge funding from the Swiss Innovation Agency Innosuisse  
656 through the Swiss Competence Centre for Energy Research – Supply of Electricity (SCCER-  
657 SoE). The HydroGIS database was provided by M. Balmer, and WASTA is updated annually by  
658 the Swiss Federal Office of Energy and made publicly available. The latest climate change  
659 scenarios were produced and made available by MeteoSwiss, and transposed into hydrological  
660 future scenarios in the framework of the Federal Office of the Environment (FOEN) programme  
661 Hydro-CH2018 (BAFU 2021).

## 662 6 References

- 663 Addor, Nans, Ole Rössler, Nina Köplin, Matthias Huss, Rolf Weingartner, and Jan Seibert.  
664 2014. "Regimes of Swiss Catchments." *Water Resources Research* 50: 7541–62.  
665 <https://doi.org/10.1002/2014WR015549>. Received.
- 666 Anderson, David, Helen Moggridge, Philip Warren, and James Shucksmith. 2015. "The Impacts  
667 of 'run-of-River' Hydropower on the Physical and Ecological Condition of Rivers." *Water  
668 and Environment Journal* 29 (2): 268–76. <https://doi.org/10.1111/wej.12101>.
- 669 BAFU. 2021. "Hydro-CH2018: Auswirkungen Des Klimawandels Auf Die Schweizer Gewässer.  
670 Hydrologie, Gewässerökologie Und Wasserwirtschaft." *Umwelt-Wissen*. Vol. Nr. 2101.  
671 Bern.
- 672 Balmer, M. 2012. *Nachhaltigkeitsbezogene Typologisierung Der Schweizerischen  
673 Wasserkraftanlagen - GIS-Basierte Clusteranalyse Und Anwendung In Einem  
674 Erfahrungskurvenmodell*. Zürich: ETHZ.
- 675 Basso, S., and G. Botter. 2012. "Streamflow Variability and Optimal Capacity of Run-of-River  
676 Hydropower Plants." *Water Resources Research* 48 (10): 1–13.  
677 <https://doi.org/10.1029/2012WR012017>.
- 678 Bejarano, M. D., A. Sordo-Ward, I. Gabriel-Martin, and L. Garrote. 2019. "Tradeoff between  
679 Economic and Environmental Costs and Benefits of Hydropower Production at Run-of-  
680 River-Diversion Schemes under Different Environmental Flows Scenarios." *Journal of  
681 Hydrology* 572 (March): 790–804. <https://doi.org/10.1016/j.jhydrol.2019.03.048>.
- 682 Bernhard, Luzi, and Massimiliano Zappa. 2009. "Schlussbericht CCHydrologie: Teilprojekt  
683 WHH-CH-Hydro. Natürlicher Wasserhaushalt Der Schweiz Und Ihre Bedeutendsten  
684 Grosseinzugsgebiete." Bern.  
685 [https://www.bafu.admin.ch/bafu/de/home/suche.html#Klimawandel Schnee Regen Eis  
686 Alpen](https://www.bafu.admin.ch/bafu/de/home/suche.html#Klimawandel%20Schnee%20Regen%20Eis%20Alpen).
- 687 ———. 2012. "Schlussbericht: CCHydrologie: Teilprojekt WHH- CH-Hydro: Natürlicher  
688 Wasserhaushalt Der Schweiz Und Ihrer Bedeutendsten Grosseinzugsgebiete."  
689 Birmensdorf.
- 690 BFE. 2020. "SCHWEIZERISCHE ELEKTRIZITÄTSSTATISTIK 2019." Bern.  
691 <https://de.statista.com/statistik/daten/studie/291824/umfrage/anzahl-der->

692 elektrowaermepumpen-in-der-schweiz/.

693 Bombelli, Giovanni Martino, Andrea Soncini, Alberto Bianchi, and Daniele Bocchiola. 2019.  
694 “Potentially Modified Hydropower Production under Climate Change in the Italian Alps.”  
695 *Hydrological Processes* 33 (17): 2355–72. <https://doi.org/10.1002/hyp.13473>.

696 Brunner, Manuela I., Astrid Björnson Gurung, Massimiliano Zappa, Harry Zekollari, Daniel  
697 Farinotti, and Manfred Stähli. 2019. “Present and Future Water Scarcity in Switzerland:  
698 Potential for Alleviation through Reservoirs and Lakes.” *Science of the Total Environment*  
699 666: 1033–47. <https://doi.org/10.1016/j.scitotenv.2019.02.169>.

700 Calapez, Ana Raquel, Sónia R.Q. Serra, Rui Rivaes, Francisca C. Aguiar, and Maria João Feio.  
701 2021. “Influence of River Regulation and Instream Habitat on Invertebrate Assemblage’  
702 Structure and Function.” *Science of the Total Environment* 794.  
703 <https://doi.org/10.1016/j.scitotenv.2021.148696>.

704 Carolli, Mauro, Carlos Garcia de Leaniz, Joshua Jones, Barbara Belletti, Helena Hudek, Martin  
705 Pusch, Pencho Pandakov, Luca Börger, and Wouter van de Bund. 2022. “Impacts of  
706 Existing and Planned Hydropower Dams on River Fragmentation in the Balkan Region.”  
707 *Science of the Total Environment* 871 (February). <https://doi.org/10.2139/ssrn.4246824>.

708 Cassagnole, Manon, Maria-Helena Ramos, Ioanna Zalachori, Guillaume Thirel, Rémy Garçon,  
709 Joël Gailhard, and Thomas Ouillon. 2020. “Impact of the Quality of Hydrological Forecasts  
710 on the Management and Revenue of Hydroelectric Reservoirs – a Conceptual Approach.”  
711 *Hydrology and Earth System Sciences Discussions*, 1–36. [https://doi.org/10.5194/hess-](https://doi.org/10.5194/hess-2020-410)  
712 2020-410.

713 CH2018. 2018. *CH2018 - Climate Scenarios for Switzerland. Technical Report*. Edited by  
714 National Centre for Climate Services. *National Centre for Climate Services*. Zurich.

715 DHI. 2004. “River Network Editor. In MIKE 11 - River Modelling Unlimited.” Hørsholm.

716 EU. 2015. *Ecological Flows in the Implementation of the Water Framework Directive: Guidance*  
717 *Document No. 31*. <https://doi.org/10.2779/775712>.

718 Farinotti, Daniel, Vanessa Round, Matthias Huss, Loris Compagno, and Harry Zekollari. 2019.  
719 “Large Hydropower and Water-Storage Potential in Future Glacier-Free Basins.” *Nature*  
720 575 (7782): 341–44. <https://doi.org/10.1038/s41586-019-1740-z>.

721 Farinotti, Daniel, Stephanie Usselman, Matthias Huss, Andreas Bauder, and Martin Funk.

722 2012. "Runoff Evolution in the Swiss Alps: Projections for Selected High-Alpine  
723 Catchments Based on ENSEMBLES Scenarios." *Hydrological Processes* 26 (13): 1909–  
724 24. <https://doi.org/10.1002/hyp.8276>.

725 Fatichi, S., S. Rimkus, P. Burlando, R. Bordoy, and P. Molnar. 2015a. "High-Resolution  
726 Distributed Analysis of Climate and Anthropogenic Changes on the Hydrology of an Alpine  
727 Catchment." *Journal of Hydrology* 525: 362–82.  
728 <https://doi.org/10.1016/j.jhydrol.2015.03.036>.

729 ———. 2015b. "High-Resolution Distributed Analysis of Climate and Anthropogenic Changes on  
730 the Hydrology of an Alpine Catchment." *Journal of Hydrology* 525: 362–82.  
731 <https://doi.org/10.1016/j.jhydrol.2015.03.036>.

732 François, B., M. Borga, S. Anquetin, J. D. Creutin, K. Engeland, A. C. Favre, B. Hingray, et al.  
733 2014. "Integrating Hydropower and Intermittent Climate-Related Renewable Energies: A  
734 Call for Hydrology." *Hydrological Processes* 28 (21): 5465–68.  
735 <https://doi.org/10.1002/hyp.10274>.

736 François, Baptiste, Benoit Hingray, Marco Borga, Davide Zoccatelli, Casey Brown, and Jean  
737 Dominique Creutin. 2018. "Impact of Climate Change on Combined Solar and Run-of-River  
738 Power in Northern Italy." *Energies* 11 (2): 1–22. <https://doi.org/10.3390/en11020290>.

739 Freudiger, Daphné, Irene Kohn, Jan Seibert, Kerstin Stahl, and Markus Weiler. 2017. "Snow  
740 Redistribution for the Hydrological Modeling of Alpine Catchments." *Wiley Interdisciplinary  
741 Reviews: Water* 4 (5): e1232. <https://doi.org/10.1002/wat2.1232>.

742 Gabbud, Chrystelle, and Stuart N. Lane. 2016. "Ecosystem Impacts of Alpine Water Intakes for  
743 Hydropower: The Challenge of Sediment Management." *Wiley Interdisciplinary Reviews:  
744 Water* 3 (1): 41–61. <https://doi.org/10.1002/wat2.1124>.

745 Gernaat, David E.H.J., Patrick W. Bogaart, Detlef P. Van Vuuren, Hester Biemans, and Robin  
746 Niessink. 2017. "High-Resolution Assessment of Global Technical and Economic  
747 Hydropower Potential." *Nature Energy* 2 (10): 821–28. [https://doi.org/10.1038/s41560-017-  
748 0006-y](https://doi.org/10.1038/s41560-017-0006-y).

749 Gorla, Lorenzo, and Paolo Perona. 2013. "On Quantifying Ecologically Sustainable Flow  
750 Releases in a Diverted River Reach." *Journal of Hydrology* 489: 98–107.  
751 <https://doi.org/10.1016/j.jhydrol.2013.02.043>.

752 GSchG. 2009. *Änderung Des Schweizer Bundesgesetz Über Den Schutz Der Gewässer*  
753 *(GSchG)*. Switzerland.  
754 <https://www.news.admin.ch/news/message/attachments/20578.pdf>.

755 ———. 2011. “Bundesgesetz Über Den Schutz Der Gewässer (Gewässerschutzgesetz  
756 *GSchG)*.” Switzerland.  
757 [https://fedlex.data.admin.ch/filestore/fedlex.data.admin.ch/eli/cc/1992/1860\\_1860\\_1860/20150908/de/pdf-a/fedlex-data-admin-ch-eli-cc-1992-1860\\_1860\\_1860-20150908-de-pdf-](https://fedlex.data.admin.ch/filestore/fedlex.data.admin.ch/eli/cc/1992/1860_1860_1860/20150908/de/pdf-a/fedlex-data-admin-ch-eli-cc-1992-1860_1860_1860-20150908-de-pdf-a.pdf)  
758 [a.pdf](https://fedlex.data.admin.ch/filestore/fedlex.data.admin.ch/eli/cc/1992/1860_1860_1860/20150908/de/pdf-a/fedlex-data-admin-ch-eli-cc-1992-1860_1860_1860-20150908-de-pdf-a.pdf).  
759

760 Gurtz, Joachim, Andri Baltensweiler, and Herbert Lang. 1999. “Spatially Distributed Hydrotope-  
761 Based Modelling of Evapotranspiration and Runoff in Mountainous Basins.” *Hydrological*  
762 *Processes* 13 (17): 2751–68.

763 HADES. 2021. “Hydrological Scenarios (Hydro-CH2018).” 2021.  
764 [https://hydromapscc.ch/#en/8/46.832/8.190/bl\\_hds--l02\\_standorte\\$0/NULL](https://hydromapscc.ch/#en/8/46.832/8.190/bl_hds--l02_standorte$0/NULL) (last accessed  
765 09 October 2021).

766 Hänggi, Pascal, and Rolf Weingartner. 2012. “Variations in Discharge Volumes for Hydropower  
767 Generation in Switzerland.” *Water Resources Management* 26 (5): 1231–52.  
768 <https://doi.org/10.1007/s11269-011-9956-1>.

769 Huss, Matthias, and Regine Hock. 2015. “A New Model for Global Glacier Change and Sea-  
770 Level Rise.” *Frontiers in Earth Science* 3 (September): 1–22.  
771 <https://doi.org/10.3389/feart.2015.00054>.

772 IEA. 2021. “Hydropower Special Market Report - Analysis and Forecast to 2030.” [www.iea.org](http://www.iea.org)  
773 (last accessed 09 March 2022).

774 IHA. 2020. “Hydropower Status Report 2020.” *International Hydropower Association*, 1–83.  
775 [https://www.hydropower.org/sites/default/files/publications-](https://www.hydropower.org/sites/default/files/publications-docs/2019_hydropower_status_report_0.pdf)  
776 [docs/2019\\_hydropower\\_status\\_report\\_0.pdf](https://www.hydropower.org/sites/default/files/publications-docs/2019_hydropower_status_report_0.pdf) (last accessed 09 March 2022).

777 Jacob, Daniela, Juliane Petersen, Bastian Eggert, Antoinette Alias, Ole Bøssing Christensen,  
778 Laurens M. Bouwer, Alain Braun, et al. 2014. “EURO-CORDEX: New High-Resolution  
779 Climate Change Projections for European Impact Research.” *Regional Environmental*  
780 *Change* 14 (2): 563–78. <https://doi.org/10.1007/s10113-013-0499-2>.

781 Kaika, Maria. 2003. “The Water Framework Directive: A New Directive for a Changing Social,

782 Political and Economic European Framework.” *European Planning Studies* 11 (3): 299–  
783 316. <https://doi.org/10.1080/09654310303640>.

784 Köplin, N., B. Schädler, D. Viviroli, and R. Weingartner. 2014. “Seasonality and Magnitude of  
785 Floods in Switzerland under Future Climate Change.” *Hydrological Processes* 28 (4):  
786 2567–78. <https://doi.org/10.1002/hyp.9757>.

787 Köplin, N., D. Viviroli, B. Schädler, and R. Weingartner. 2010. “How Does Climate Change  
788 Affect Mesoscale Catchments in Switzerland? - A Framework for a Comprehensive  
789 Assessment.” *Advances in Geosciences* 27: 111–19. [https://doi.org/10.5194/adgeo-27-  
790 111-2010](https://doi.org/10.5194/adgeo-27-111-2010).

791 Kuriqi, Alban, António N. Pinheiro, Alvaro Sordo-Ward, María D. Bejarano, and Luis Garrote.  
792 2021. “Ecological Impacts of Run-of-River Hydropower Plants—Current Status and Future  
793 Prospects on the Brink of Energy Transition.” *Renewable and Sustainable Energy Reviews*  
794 142 (March): 17. <https://doi.org/10.1016/j.rser.2021.110833>.

795 Kuriqi, Alban, António N. Pinheiro, Alvaro Sordo-Ward, and Luis Garrote. 2019. “Flow Regime  
796 Aspects in Determining Environmental Flows and Maximising Energy Production at Run-of-  
797 River Hydropower Plants.” *Applied Energy* 256 (October).  
798 <https://doi.org/10.1016/j.apenergy.2019.113980>.

799 Laufer, Fred, Stephan Grötzinger, Marco Peter, and Alain Schmutz. 2004. “Ausbaupotential Der  
800 Wasserkraft.” Bern. <https://www.news.admin.ch/news/message/attachments/2663.pdf>.

801 Mohor, Guilherme Samprogná, Daniel Andrés Rodríguez, Javier Tomasella, and José Lázaro  
802 Siqueira Júnior. 2015. “Exploratory Analyses for the Assessment of Climate Change  
803 Impacts on the Energy Production in an Amazon Run-of-River Hydropower Plant.” *Journal  
804 of Hydrology: Regional Studies* 4 (PB): 41–59. <https://doi.org/10.1016/j.ejrh.2015.04.003>.

805 Muelchi, Regula, Ole Rössler, Jan Schwanbeck, Rolf Weingartner, and Olivia Martius. 2021.  
806 “River Runoff in Switzerland in a Changing Climate - Changes in Moderate Extremes and  
807 Their Seasonality.” *Hydrology and Earth System Sciences* 25 (6): 3577–94.  
808 <https://doi.org/10.5194/hess-25-3577-2021>.

809 Quaranta, Emanuele, Amir Bahreini, Alireza Riasi, and Roberto Revelli. 2022. “The Very Low  
810 Head Turbine for Hydropower Generation in Existing Hydraulic Infrastructures: State of the  
811 Art and Future Challenges.” *Sustainable Energy Technologies and Assessments* 51 (June  
812 2021): 101924. <https://doi.org/10.1016/j.seta.2021.101924>.

813 Ranzani, Alessandro, Mattia Bonato, Epari Ritesh Patro, Ludovic Gaudard, and Carlo De  
814 Michele. 2018. "Hydropower Future: Between Climate Change, Renewable Deployment,  
815 Carbon and Fuel Prices." *Water (Switzerland)* 10 (9): 1–17.  
816 <https://doi.org/10.3390/w10091197>.

817 RGI Consortium. 2017. "Randolph Glacier Inventory –A Dataset of Global Glacier Outlines:  
818 Version 6.0: Technical Report, Global Land Ice Measurements from Space." Colorado.  
819 <https://doi.org/https://doi.org/10.7265/N5-RGI-60>.

820 Savelsberg, Jonas, Moritz Schillinger, Ingmar Schlecht, and Hannes Weigt. 2018. "The Impact  
821 of Climate Change on Swiss Hydropower." *Sustainability (Switzerland)* 10 (7): 23.  
822 <https://doi.org/10.3390/su10072541>.

823 Schaefli, Bettina, Pedro Manso, Mauro Fischer, Matthias Huss, and Daniel Farinotti. 2019. "The  
824 Role of Glacier Retreat for Swiss Hydropower Production." *Renewable Energy* 132: 615–  
825 27. <https://doi.org/10.1016/j.renene.2018.07.104>.

826 Schattan, Paul, Massimiliano Zappa, Heike Lischke, Luzi Bernhard, Esther Thürig, and Bernd  
827 Diekkrüger. 2013. "An Approach for Transient Consideration of Forest Change in  
828 Hydrological Impact Studies." *IAHS-AISH Proceedings and Reports* 359 (July): 311–19.

829 Skjelbred, H. I., and J. Kong. 2019. "A Comparison of Linear Interpolation and Spline  
830 Interpolation for Turbine Efficiency Curves in Short-Term Hydropower Scheduling  
831 Problems." *IOP Conference Series: Earth and Environmental Science* 240 (4).  
832 <https://doi.org/10.1088/1755-1315/240/4/042011>.

833 Speich, Matthias J.R., Luzi Bernhard, Adriaan J. Teuling, and Massimiliano Zappa. 2015.  
834 "Application of Bivariate Mapping for Hydrological Classification and Analysis of Temporal  
835 Change and Scale Effects in Switzerland." *Journal of Hydrology* 523: 804–21.  
836 <https://doi.org/10.1016/j.jhydrol.2015.01.086>.

837 Temel, Pelin, Elcin Kentel, Emre Alp, and Emre Alp. 2023. "Development of a Site Selection  
838 Methodology for Run-of-River Hydroelectric Power Plants within the Water-Energy-  
839 Ecosystem Nexus." *Science of the Total Environment* 856 (September 2022): 159152.  
840 <https://doi.org/10.1016/j.scitotenv.2022.159152>.

841 Totschnig, G., R. Hirner, A. Müller, L. Kranzl, M. Hummel, H. P. Nachtnebel, P. Stanzel, I.  
842 Schicker, and H. Formayer. 2017. "Climate Change Impact and Resilience in the Electricity  
843 Sector: The Example of Austria and Germany." *Energy Policy* 103 (January): 238–48.

- 844 <https://doi.org/10.1016/j.enpol.2017.01.019>.
- 845 Vázquez-Tarrío, Daniel, Michal Tal, Benoît Camenen, and Hervé Piégay. 2019. "Effects of  
846 Continuous Embankments and Successive Run-of-the-River Dams on Bedload Transport  
847 Capacities along the Rhône River, France." *Science of the Total Environment* 658: 1375–  
848 89. <https://doi.org/10.1016/j.scitotenv.2018.12.109>.
- 849 Viviroli, Daniel, Heidi Mittelbach, Joachim Gurtz, and Rolf Weingartner. 2009. "Continuous  
850 Simulation for Flood Estimation in Ungauged Mesoscale Catchments of Switzerland - Part  
851 II: Parameter Regionalisation and Flood Estimation Results." *Journal of Hydrology* 377 (1–  
852 2): 208–25. <https://doi.org/10.1016/j.jhydrol.2009.08.022>.
- 853 Viviroli, Daniel, Massimiliano Zappa, Joachim Gurtz, and Rolf Weingartner. 2009. "An  
854 Introduction to the Hydrological Modelling System PREVAH and Its Pre- and Post-  
855 Processing-Tools." *Environmental Modelling and Software* 24 (10): 1209–22.  
856 <https://doi.org/10.1016/j.envsoft.2009.04.001>.
- 857 Viviroli, Daniel, Massimiliano Zappa, Jan Schwanbeck, Joachim Gurtz, and Rolf Weingartner.  
858 2009. "Continuous Simulation for Flood Estimation in Ungauged Mesoscale Catchments of  
859 Switzerland - Part I: Modelling Framework and Calibration Results." *Journal of Hydrology*  
860 377 (1–2): 191–207. <https://doi.org/10.1016/j.jhydrol.2009.08.023>.
- 861 Vogel, Richard M, and Neil M Fennessey. 1995. "FLOW DURATION CURVES II : A REVIEW  
862 OF APPLICATIONS IN WATER RESOURCES PLANNING ' Proverb " One Picture Is  
863 Worth a Thousand Words " Are Used to Summarize the Results of Detailed and Ly ,  
864 Streamfiow Duration Curves Have Been Used in Sparse . This Is the Fir." *Water Resources*  
865 *Bulletin* 31 (6): 1029–39.
- 866 Wagner, T., M. Themeßl, A. Schüppel, A. Gobiet, H. Stigler, and S. Birk. 2017. "Impacts of  
867 Climate Change on Stream Flow and Hydro Power Generation in the Alpine Region."  
868 *Environmental Earth Sciences* 76 (1). <https://doi.org/10.1007/s12665-016-6318-6>.
- 869 WASTA. 2019. "Statistik Der Wasserkraftanlagen Der Schweiz ( WASTA )." Bern: Bundesamt  
870 für Energie (BFE).
- 871 Wechsler, Tobias. 2021. "RoRCC." Zurich: Envidat. <https://doi.org/10.16904/envidat.259>.
- 872 Wechsler, Tobias, Massimiliano Zappa, and Andreas Inderwildi. 2021. "In Publication:  
873 Projektbericht: Auswirkungen Klimaszenarien CH2018 Auf Alpenrandseen." Bern.



874 Westerberg, I. K., J. L. Guerrero, P. M. Younger, K. J. Beven, J. Seibert, S. Halldin, J. E. Freer,  
875 and C. Y. Xu. 2011. "Calibration of Hydrological Models Using Flow-Duration Curves."  
876 *Hydrology and Earth System Sciences* 15 (7): 2205–27. [https://doi.org/10.5194/hess-15-](https://doi.org/10.5194/hess-15-2205-2011)  
877 [2205-2011](https://doi.org/10.5194/hess-15-2205-2011).

878 Yildiz, Veysel, and Jasper A. Vrugt. 2019. "A Toolbox for the Optimal Design of Run-of-River  
879 Hydropower Plants." *Environmental Modelling and Software* 111 (January): 134–52.  
880 <https://doi.org/10.1016/j.envsoft.2018.08.018>.

881 Zekollari, Harry, Matthias Huss, and Daniel Farinotti. 2019. "Modelling the Future Evolution of  
882 Glaciers in the European Alps under the EURO-CORDEX RCM Ensemble." *Cryosphere* 13  
883 (4): 1125–46. <https://doi.org/10.5194/tc-13-1125-2019>.

884

885 **1 Supplementary Information**

886 **1.1 Climate change scenarios CH2018**

887 *Table SI1. The 39 climate model ensembles used in this study are based on the CH2018 climate scenarios (CH2018*  
 888 *2018). The combination of TEAM (responsible institute), RCM (Regional Climate Model), GCM (General Circulation*  
 889 *Models), RES (spatial resolution), and RCP (Representative Concentration Pathway = emissions scenario) is shown*  
 890 *for each ensemble. The colours correspond to the three RCPs (RCP2.6, RCP4.5, RCP8.5).*

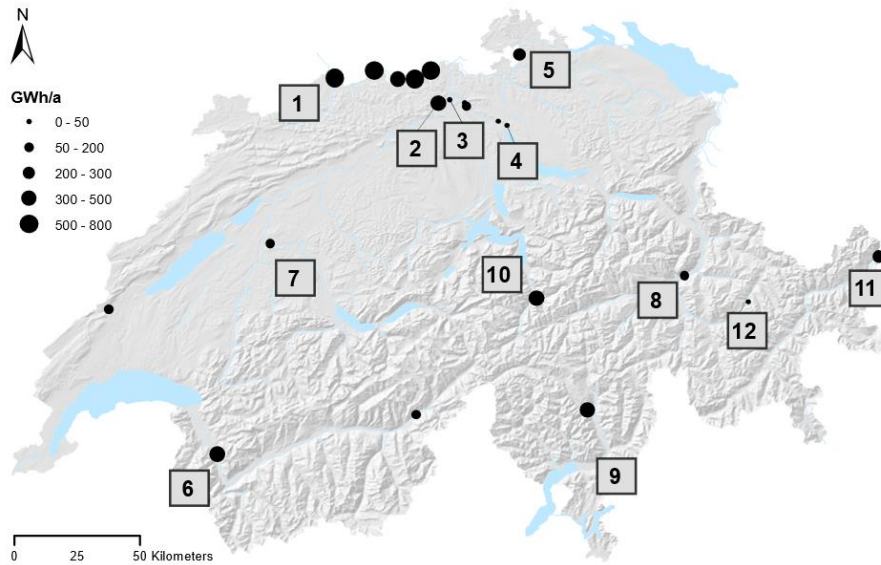
TEAM	RCM	GCM	RES	RCP	TEAM	RCM	GCM	RES	RCP
DMI	HIRHAM	ECEARTH	EUR11	RCP2.6	CLMCOM	CCLM4	HADGEM	EUR44	RCP8.5
KNMI	RACMO	HADGEM	EUR44	RCP2.6	CLMCOM	CCLM5	ECEARTH	EUR44	RCP8.5
SMHI	RCA	ECEARTH	EUR11	RCP2.6	CLMCOM	CCLM5	HADGEM	EUR44	RCP8.5
SMHI	RCA	ECEARTH	EUR44	RCP2.6	CLMCOM	CCLM5	MIROC	EUR44	RCP8.5
SMHI	RCA	HADGEM	EUR44	RCP2.6	CLMCOM	CCLM5	MPIESM	EUR44	RCP8.5
SMHI	RCA	MIROC	EUR44	RCP2.6	DMI	HIRHAM	ECEARTH	EUR11	RCP8.5
SMHI	RCA	MPIESM	EUR44	RCP2.6	DMI	HIRHAM	ECEARTH	EUR44	RCP8.5
SMHI	RCA	NORESM	EUR44	RCP2.6	KNMI	RACMO	ECEARTH	EUR44	RCP8.5
DMI	HIRHAM	ECEARTH	EUR11	RCP4.5	KNMI	RACMO	HADGEM	EUR44	RCP8.5
DMI	HIRHAM	ECEARTH	EUR44	RCP4.5	SMHI	RCA	CCCMA	EUR44	RCP8.5
KNMI	RACMO	ECEARTH	EUR44	RCP4.5	SMHI	RCA	ECEARTH	EUR11	RCP8.5
KNMI	RACMO	HADGEM	EUR44	RCP4.5	SMHI	RCA	ECEARTH	EUR44	RCP8.5
SMHI	RCA	CCCMA	EUR44	RCP4.5	SMHI	RCA	HADGEM	EUR11	RCP8.5
SMHI	RCA	ECEARTH	EUR11	RCP4.5	SMHI	RCA	HADGEM	EUR44	RCP8.5
SMHI	RCA	ECEARTH	EUR44	RCP4.5	SMHI	RCA	MIROC	EUR44	RCP8.5
SMHI	RCA	HADGEM	EUR11	RCP4.5	SMHI	RCA	MPIESM	EUR11	RCP8.5
SMHI	RCA	HADGEM	EUR44	RCP4.5	SMHI	RCA	MPIESM	EUR44	RCP8.5
SMHI	RCA	MIROC	EUR44	RCP4.5	SMHI	RCA	NORESM	EUR44	RCP8.5
SMHI	RCA	MPIESM	EUR11	RCP4.5					
SMHI	RCA	MPIESM	EUR44	RCP4.5					
SMHI	RCA	NORESM	EUR44	RCP4.5					

891

## 892 1.2 Model calibration

893 *Table SI2. Results of the calibration and verification by Bernhard and Zappa (2012) and Speich et al. (2015) of the*  
 894 *hydrological modelled discharge at selected stations (Figure SI1) for the calibration period (1984–1996) and verification*  
 895 *periods (1980–1983 & 1997–2009). Nr. corresponds to the number in Figure SI1; Name indicates the name of the*  
 896 *discharge measurement station; Cal/Val indicate calibration and validation; NS is the Nash criterion [no unit]; NSL is*  
 897 *the logarithmic Nash criterion [no unit]; DV is the volume error [%]. The link is to the web atlas (HADES 2021) where*  
 898 *the streamflow regimes and hydrological future projections are visualised.*

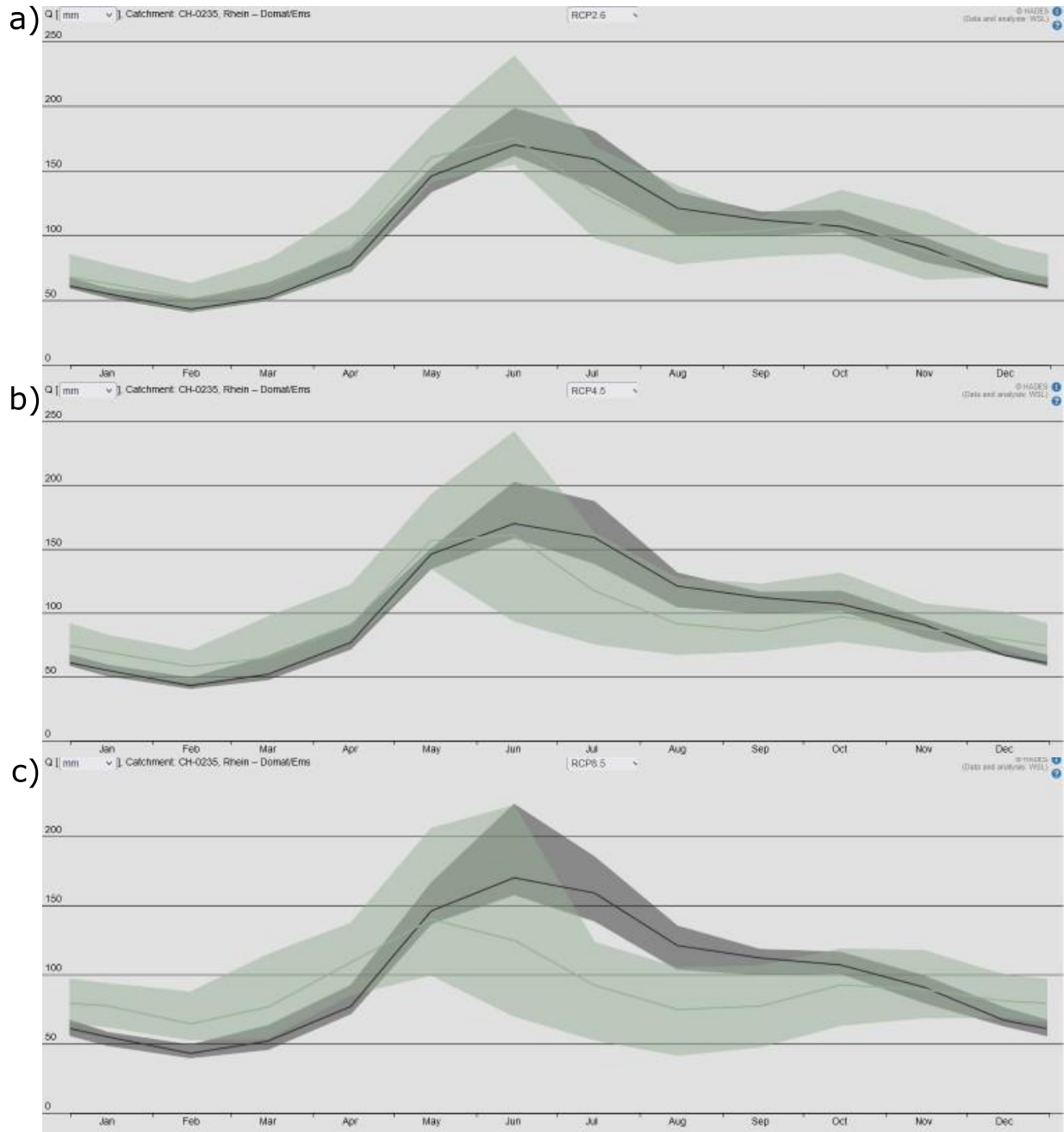
Nr.	Name	Cal/Val	NS	NSL	DV	Link
1	Rhine, Basel	Cal	0.953	0.95	0.3	<a href="https://hydromapscc.ch/#en/9/47.3379/7.8662/bl_hds--l02_standorte\$CH-0146+0/NULL">https://hydromapscc.ch/#en/9/47.3379/7.8662/bl_hds--l02_standorte\$CH-0146+0/NULL</a>
		Val	0.927	0.931	-3.4	
2	Aare, Brugg	Cal	0.9	0.9	-0.9	<a href="https://hydromapscc.ch/#en/10/47.2657/8.2892/bl_hds--l01_standorte\$CH-0200--l02_standorte\$CH-0064+0/NULL">https://hydromapscc.ch/#en/10/47.2657/8.2892/bl_hds--l01_standorte\$CH-0200--l02_standorte\$CH-0064+0/NULL</a>
		Val	0.883	0.887	-2.7	
3	Reuss, Mellingen	Cal	0.932	0.918	-1.8	<a href="https://hydromapscc.ch/#en/11/47.2795/8.4512/bl_hds--l02_standorte\$CH-0051+0/NULL">https://hydromapscc.ch/#en/11/47.2795/8.4512/bl_hds--l02_standorte\$CH-0051+0/NULL</a>
		Val	0.919	0.902	-2.2	
4	Limmatt, Unterhard	Cal	0.9	0.885	-0.3	<a href="https://hydromapscc.ch/#en/10/47.2191/8.5625/bl_hds--l02_standorte\$CH-0075+0/NULL">https://hydromapscc.ch/#en/10/47.2191/8.5625/bl_hds--l02_standorte\$CH-0075+0/NULL</a>
		Val	0.883	0.874	-2.2	
5	Rhein, Neuhausen	Cal	0.954	0.935	2.6	<a href="https://hydromapscc.ch/#en/9/47.5367/8.8770/bl_hds--l02_standorte\$CH-0145+0/NULL">https://hydromapscc.ch/#en/9/47.5367/8.8770/bl_hds--l02_standorte\$CH-0145+0/NULL</a>
		Val	0.903	0.898	-2.4	
6	Rhone, Porte	Cal	0.529	0.449	5.2	<a href="https://hydromapscc.ch/#en/9/46.5787/7.4899/bl_hds--l02_standorte\$CH-0047+0/NULL">https://hydromapscc.ch/#en/9/46.5787/7.4899/bl_hds--l02_standorte\$CH-0047+0/NULL</a>
		Val	0.571	0.523	3.2	
7	Aare, Schoenau	Cal	0.897	0.895	-1.6	<a href="https://hydromapscc.ch/#en/9/46.5787/7.4927/bl_hds--l02_standorte\$CH-0092+0/NULL">https://hydromapscc.ch/#en/9/46.5787/7.4927/bl_hds--l02_standorte\$CH-0092+0/NULL</a>
		Val	0.907	0.911	-3.3	
8	Rhein, Domat, Ems	Cal	0.752	0.635	5.7	<a href="https://hydromapscc.ch/#en/9/46.8949/9.0720/bl_hds--l02_standorte\$CH-0235+0/NULL">https://hydromapscc.ch/#en/9/46.8949/9.0720/bl_hds--l02_standorte\$CH-0235+0/NULL</a>
		Val	0.782	0.682	0.7	
9	Ticino, Bellinzona	Cal	0.793	0.735	0.7	<a href="https://hydromapscc.ch/#en/10/46.2848/9.1544/bl_hds--l02_standorte\$CH-0053+0/NULL">https://hydromapscc.ch/#en/10/46.2848/9.1544/bl_hds--l02_standorte\$CH-0053+0/NULL</a>
		Val	0.816	0.698	-2.5	
10	Reuss, Seedorf	Cal	0.857	0.778	-0.3	<a href="https://hydromapscc.ch/#en/10/46.7667/8.6215/bl_hds--l02_standorte\$CH-0138--l01_standorte\$CH-0061+0/NULL">https://hydromapscc.ch/#en/10/46.7667/8.6215/bl_hds--l02_standorte\$CH-0138--l01_standorte\$CH-0061+0/NULL</a>
		Val	0.821	0.779	-3.3	
11	Inn, Martina	Cal	0.727	0.645	-3.6	<a href="https://hydromapscc.ch/#en/8/46.840/10.563/bl_hds--l02_standorte\$CH-0289+0/NULL">https://hydromapscc.ch/#en/8/46.840/10.563/bl_hds--l02_standorte\$CH-0289+0/NULL</a>
		Val	0.732	0.698	-8.0	
12	Landwasser, Davos	Cal	0.862	0.919	6.8	<a href="https://hydromapscc.ch/#en/10/46.7093/10.1376/bl_hds--l02_standorte\$CH-0138--l01_standorte\$CH-0169+0/NULL">https://hydromapscc.ch/#en/10/46.7093/10.1376/bl_hds--l02_standorte\$CH-0138--l01_standorte\$CH-0169+0/NULL</a>
		Val	0.851	0.884	2.9	



900

901 *Figure S11. The 21 Swiss run-of-river power plants considered in this study. The size of the dots represents the annual*  
 902 *production in GWh a<sup>-1</sup>. The numbers correspond to the discharge measuring stations in Table S12 that were used for*  
 903 *calibration and validation.*

904 1.3 Hydrological regimes



905

906 *Figure SI2. Changes in mean monthly streamflow under the three emissions scenarios a) RCP2.6, b) RCP4.5, and c)*  
907 *RCP8.5 by the end of the century (2070–2099, green) in comparison to the reference period (1981–2010, black) at*  
908 *Domat Ems (Nr. 8 in Table SI2 and Figure SI1) shown at <https://hydromapscc.ch>.*

909

#### 910 1.4 Hydrological scenarios CH2018

911 PREVAH is a conceptual, process-oriented model (Viviroli et al. 2009), which has been  
912 continuously improved since its development (Gurtz et al. 1999). As part of the CCHydro study  
913 (Bernhard and Zappa 2012), a spatially explicit (grid) version was created for PREVAH, with a  
914 resolution of 200 m × 200 m (Schattan et al. 2013; Speich et al. 2015; Brunner et al. 2019).  
915 PREVAH consists of several model components covering the following hydrological processes  
916 (Viviroli et al. 2009): interception, evapotranspiration, snow accumulation and melt, glacier melt,  
917 soil water storage evolution, groundwater recharge and ensuing baseflow, surface and  
918 subsurface discharge formation, and discharge transfer. The model parameters have already  
919 been calibrated, validated and regionalised (Viviroli et al. 2009; Viviroli et al. 2009; Köplin et al.  
920 2010; Bernhard and Zappa 2012; Speich et al. 2015). The digital elevation model (DEM), land-  
921 use data, glacier inventory and meteorological data are then inserted as inputs into the calibrated  
922 model (Brunner et al. 2019). The meteorological data are spatially interpolated by inverse distance  
923 weighting (IDW) and a combination of IDW and elevation dependent regression (EDR; Viviroli et  
924 al. 2009; Bernhard and Zappa 2012). Snow accumulation and melting in PREVAH are determined  
925 by temperature and global radiation (Viviroli et al. 2009). Compared with early applications, the  
926 model version underlying the present scenarios has been improved with regard to the  
927 representation of snow accumulation at high elevations (Freudiger et al. 2017) and to the  
928 representation of glaciers and their length evolution (Brunner et al. 2019). Only a certain amount  
929 of snow can accumulate per grid cell, which depends on the slope of the terrain. Excess snow is  
930 then relocated, based on the DEM, to lower elevations where snowmelt is more likely. The glaciers  
931 are divided into short (< 1 km) and long glaciers (> 1 km) (RGI Consortium 2017). The future  
932 glacier extent is modelled with the Global Glacier Evolution Model (GloGEM) for short glaciers  
933 (Huss and Hock 2015) and with the newer, extended version of GloGEM (GloGEMflow) for long  
934 glaciers (Zekollari et al. 2019). The simulated glacier lengths are finally converted to the PREVAH  
935 model grid (Brunner et al. 2019; Zekollari et al. 2019). In addition to incorporating the mass

936 balance due to freezing and thawing at the glacier surface, the model considers changes due to  
937 glacier flow. The resulting melt-water quantities are determined from the changes in the glacier  
938 surfaces over intervals of 5 years and fed into the precipitation-discharge model. For Lake Zurich,  
939 an interface with the hydrodynamic model Mike11 (DHI 2004) has been created to take lake  
940 regulation into account (Wechsler et al. 2021).